

Locally adaptive factor processes for multivariate time series

Daniele Durante

*Department of Statistical Sciences
University of Padua
Padua, Italy*

DURANTE@STAT.UNIPD.IT

Bruno Scarpa

*Department of Statistical Sciences
University of Padua
Padua, Italy*

SCARPA@STAT.UNIPD.IT

David B. Dunson

*Department of Statistical Science
Duke University
Durham, NC 27708-0251, USA*

DUNSON@STAT.DUKE.EDU

Editor:

Abstract

1 In modeling multivariate time series, it is important to allow time-varying smoothness in the
 2 mean and covariance process. In particular, there may be certain time intervals exhibiting
 3 rapid changes and others in which changes are slow. If such time-varying smoothness is not
 4 accounted for, one can obtain misleading inferences and predictions, with over-smoothing
 5 across erratic time intervals and under-smoothing across times exhibiting slow variation.
 6 This can lead to mis-calibration of predictive intervals, which can be substantially too
 7 narrow or wide depending on the time. We propose a locally adaptive factor process for
 8 characterizing multivariate mean-covariance changes in continuous time, allowing locally
 9 varying smoothness in both the mean and covariance matrix. This process is constructed
 10 utilizing latent dictionary functions evolving in time through nested Gaussian processes and
 11 linearly related to the observed data with a sparse mapping. Using a differential equation
 12 representation, we bypass usual computational bottlenecks in obtaining MCMC and online
 13 algorithms for approximate Bayesian inference. The performance is assessed in simulations
 14 and illustrated in a financial application.

15 **Keywords:** Bayesian nonparametrics; locally varying smoothness; long-range depen-
 16 dence; multivariate time series; nested Gaussian process; stochastic volatility.

17 1. Introduction

18 1.1 Motivation and setting

19 In analyzing multivariate time series data, collected in financial applications, monitoring of
 20 influenza outbreaks and other fields, it is often of key importance to accurately characterize
 21 dynamic changes over time in not only the mean of the different elements (e.g., assets,
 22 influenza levels at different locations) but also the covariance. As shown in Figure 1, it
 23 is typical in many domains to cycle irregularly between periods of rapid and slow change;
 24 most statistical models are insufficiently flexible to capture such locally varying smoothness

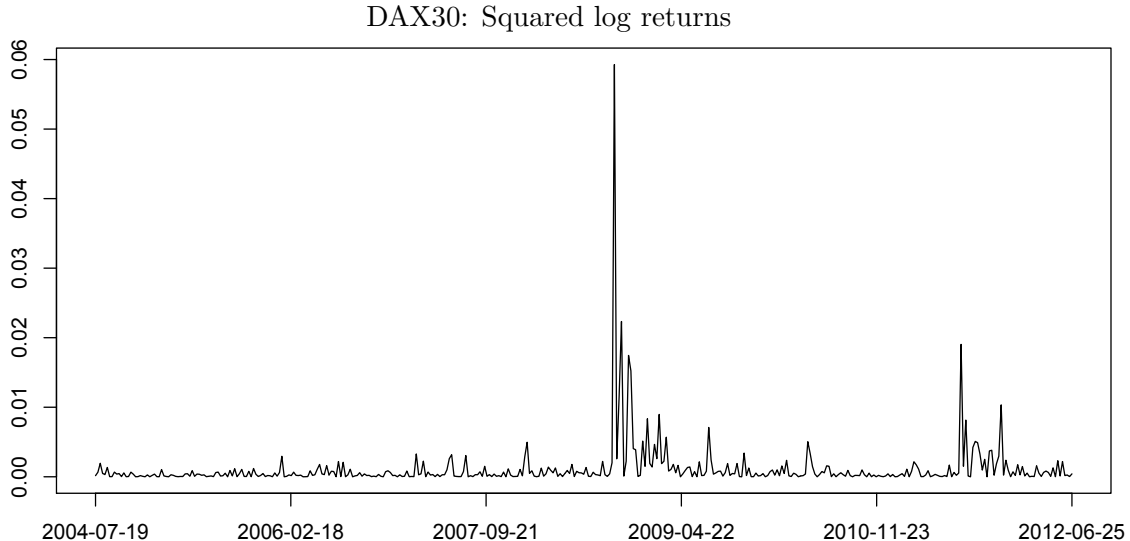


Figure 1: Squared Log>Returns of DAX30, using weekly data from 2004/07/19, to 2012/06/25.

25 in assuming a single bandwidth parameter. Inappropriately restricting the smoothness to
 26 be constant can have a major impact on the quality of inferences and predictions, with over-
 27 smoothing occurring during times of rapid change. This leads to an under-estimation of
 28 uncertainty during such volatile times and an inability to accurately predict risk of extremal
 29 events.

30 Let $Y_t = (Y_{t1}, \dots, Y_{tp})^T$ denote a random vector at time t , with $\mu(t) = E(Y_t)$ and
 31 $\Sigma(t) = \text{cov}(Y_t)$. Our focus is on Bayesian modeling and inference for the multivariate mean-
 32 covariance stochastic process, $\Gamma = \{\mu(t), \Sigma(t), t \in \mathcal{T}\}$ with $\mathcal{T} \subset \mathbb{R}_+$. Of particular interest
 33 is allowing locally-varying smoothness, meaning that the rate of change in the $\{\mu(t), \Sigma(t)\}$
 34 process is varying over time. To our knowledge, there is no previous proposed stochastic
 35 process for a coupled mean-covariance process, which allows locally-varying smoothness. A
 36 key to our construction is the use of latent processes, which have time-varying smoothness.
 37 This results in a *locally adaptive factor* (LAF) process. We review the relevant literature
 38 below and then describe our LAF formulation.

39 1.2 Relevant literature

40 There is a rich literature on modeling a $p \times 1$ time-varying mean vector $\mu(t)$, covering
 41 multivariate generalizations of autoregressive models (VAR, e.g. Tsay, 2005), Kalman fil-
 42 tering (Kalman, 1960), nonparametric mean regression via Gaussian processes (GP) (Ras-
 43 mussen and Williams, 2006), polynomial spline (Huang, Wu and Zhou, 2002), smoothing
 44 spline (Hastie and Tibshirani, 1990) and kernel smoothing methods (Wolpert, Clyde and
 45 Tu, 2011). Such approaches perform well for slowly-changing trajectories with constant

46 bandwidth parameters regulating implicitly or explicitly global smoothness; however, our
 47 interest is allowing smoothness to vary locally in continuous time. Possible extensions for
 48 local adaptivity include free knot splines (MARS) (Friedman, 1991), which perform well in
 49 simulations but the different strategies proposed to select the number and the locations of
 50 knots (stepwise knot selection (Friedman, 1991), Bayesian knot selection (Smith and Kohn,
 51 1996) or via MCMC methods (George and McCulloch, 1993)) prove to be computationally
 52 intractable for moderately large p . Other flexible approaches include wavelet shrinkage
 53 (Donoho and Johnstone, 1995), local polynomial fitting via variable bandwidth (Fan and
 54 Gijbels, 1995) and linear combination of kernels with variable bandwidths (Wolpert, Clyde
 55 and Tu, 2011).

56 There is a separate literature on estimating a time-varying covariance matrix $\Sigma(t)$. This
 57 is particular of interest in applications where volatilities and co-volatilities evolve through
 58 non constant paths. One popular approach estimates $\Sigma(t)$ via an exponentially weighted
 59 moving average (EWMA; see, e.g., Tsay, 2005). This approach uses a single time-constant
 60 smoothing parameter $0 < \lambda < 1$, with extensions to accommodate locally-varying smooth-
 61 ness not straightforward due to the need to maintain positive semidefinite $\Sigma(t)$ at every
 62 time. To allow for higher flexibility in the dynamic of the covariances, generalizations of
 63 EWMA have been proposed including the diagonal vector ARCH model (DVEC), (Bollers-
 64 levs, Engle and Wooldridge, 1988) and its variant, the BEKK model (Engle and Kroner,
 65 1995). These models are computationally demanding and are not designed for moderate to
 66 large p . DCC-GARCH (Engle, 2002) improves the computational tractability of the previ-
 67 ous approaches through a two-step formulation. However, the univariate GARCH assumed
 68 for the conditional variances of each time series and the higher level GARCH models with
 69 the same parameters regulating the evolution of the time varying conditional correlations,
 70 restrict the evolution of the variance and covariance matrices. PC-GARCH (Ding, 1994 and
 71 Burns, 2005) and O-GARCH (Alexander, 2001) perform dimensionality reduction through
 72 a latent factor formulation (see also van der Wiede, 2002). However, time-constant factor
 73 loadings and uncorrelated latent factors constrain the evolution of $\Sigma(t)$.

74 Such models fall far short of our goal of allowing $\Sigma(t)$ to be fully flexible with the
 75 dependence between $\Sigma(t)$ and $\Sigma(t + \Delta)$ varying with not just the time-lag Δ but also with
 76 time. In addition, these models do not handle missing data easily and tend to require long
 77 series for accurate estimation (Burns, 2005). Accommodating changes in continuous time
 78 is important in many applications, and avoids having the model be critically dependent on
 79 the time scale, with inconsistent models obtained as time units are varied.

80 Wilson and Ghahramani (2010) join machine learning and econometrics efforts by propos-
 81 ing a model for both mean and covariance regression in multivariate time series, improving
 82 previous work of Bru (1991) on Wishart processes in terms of computational tractability
 83 and scalability, allowing a more complex structure of dependence between $\Sigma(t)$ and $\Sigma(t + \Delta)$.
 84 Specifically, they propose a continuous time Generalised Wishart Process (GWP), which
 85 defines a collection of positive semi-definite random matrices $\Sigma(t)$ with Wishart marginals.
 86 Nonparametric mean regression for $\mu(t)$ is also considered via GP priors; however, the tra-
 87 jectories of means and covariances inherit the smooth behavior of the underlying Gaussian
 88 processes, limiting the flexibility of the approach in times exhibiting sharp changes.

89 Even for iid observations from a multivariate normal model with a single time stationary
 90 covariance matrix, there are well known problems with Wishart priors motivating a rich

91 literature on dimensionality reduction techniques based on factor and graphical models.
 92 There has been abundant recent interest in applying such approaches to dynamic settings.
 93 Refer to Nakajima and West (2012) and the references cited therein for recent literature
 94 on Bayesian dynamic factor models for multivariate stochastic volatility. Their approach
 95 allows the factor loadings to evolve dynamically over time, while including sparsity through
 96 a latent thresholding approach, leading to apparently improved performance in portfolio
 97 allocation. They utilize a time-varying discrete-time autoregressive model, which allows
 98 the dependence in the covariance matrices $\Sigma(t)$ and $\Sigma(t + \Delta)$ to vary as a function of both
 99 t and Δ . However, the result is an extremely richly parameterized and computationally
 100 challenging model, with selection of the number of factors proceeding by cross validation.
 101 Our emphasis is instead on developing continuous time stochastic processes for $\Sigma(t)$ and
 102 $\mu(t)$, which accommodate locally-varying smoothness.

103 Fox and Dunson (2011) propose an alternative Bayesian covariance regression (BCR)
 104 model, which defines the covariance matrix as a regularized quadratic function of time-
 105 varying loadings in a latent factor model, characterizing the latter as a sparse combination
 106 of a collection of unknown Gaussian process (GP) dictionary functions. Although their
 107 approach provides a continuous time and highly flexible model that accommodates miss-
 108 ing data and scales to moderately large p , there are two limitations motivating this article.
 109 Firstly, their proposed covariance stochastic process assumes a stationary dependence struc-
 110 ture, and hence tends to under-smooth during periods of stability and over-smooth during
 111 periods of sharp changes. Secondly, the well known computational problems with usual GP
 112 regression are inherited, leading to difficulties in scaling to long series and issues in mixing
 113 of MCMC algorithms for posterior computation.

114 1.3 Contribution and outline

115 Our proposed LAF process instead includes dictionary functions that are generated from
 116 nested Gaussian processes (nGP) (Zhu and Dunson, 2012). Such nGP reduces the GP com-
 117 putational burden involving matrix inversions from $O(T^3)$ to $O(T)$, with T denoting the
 118 length of the time series, while also allowing flexible locally-varying smoothness. Marginal-
 119 izing out the latent factors, we obtain a stochastic process that inherits these advantages.
 120 We also develop a different and more computationally efficient approach to computation un-
 121 der this new model and propose online implementation, which can accommodate streaming
 122 data. In Section 2, we describe LAF structure with particular attention to prior specifica-
 123 tion. Section 3 explores the main features of the Gibbs sampler for posterior computation
 124 and outlines the steps for a fast online updating approach. In Section 4 we compare our
 125 model to BCR and to some of the most quoted models for multivariate stochastic volatility,
 126 through simulation studies. Finally in Section 5 an application to stock market indices
 127 across countries is examined.

128 2. Locally Adaptive Factor Processes

129 2.1 Notation and motivation

130 Our focus is on defining a novel locally adaptive factor (LAF) process for $\Gamma = \{\mu(t), \Sigma(t), t \in$
 131 $\mathcal{T}\}$. In particular, taking a Bayesian approach, we define a prior $\Gamma \sim P$, where P is a

132 probability measure over the space \mathcal{P} of p -variate mean-covariance processes on \mathcal{T} . In
 133 particular, each element of \mathcal{P} corresponds to a realization of the stochastic process Γ , and
 134 the measure P assigns probabilities to a σ -algebra of subsets of \mathcal{P} .

135 Although the proposed class of LAF processes can be used much more broadly, in
 136 conducting inferences in this article, we focus on the simple case in which data consist
 137 of vectors $y_i = (y_{i1}, \dots, y_{ip})^T$ collected at times t_i , for $i = 1, \dots, n$. These times can be
 138 unequally-spaced, or collected under an equally-spaced design with missing observations.
 139 An advantage of using a continuous-time process is that it is trivial to allow unequal spacing,
 140 missing data, and even observation times across which only a subset of the elements of y_i
 141 are observed. We additionally make the simplifying assumption that

$$Y_i \sim N_p(\mu(t_i), \Sigma(t_i)).$$

142 It is straightforward to modify the methodology to accommodate substantially different
 143 observation models.

144 2.2 LAF specification

145 A common strategy in modeling of large p matrices is to rely on a lower-dimensional fac-
 146 torization, with factor analysis providing one possible direction. Sparse Bayesian factor
 147 models have been particularly successful in challenging cases, while having advantages over
 148 frequentist competitors in incorporating a probabilistic characterization of uncertainty in
 149 the number of factors as well as the parameters in the loadings and residual covariance. For
 150 recent articles on Bayesian sparse factor analysis for a single large covariance matrix, refer
 151 to Bhattacharya and Dunson (2011), Pati et al. (2012) and the references cited there-in.

152 In our setting, we are instead interested in letting the mean vector and the covariance
 153 matrix vary flexibly over time. Extending the usual factor analysis framework to this setting,
 154 we say that $\Gamma = \{\mu(t), \Sigma(t), t \in \mathcal{T}\} \sim \text{LAF}_{L,K}(\Theta, \Sigma_0, \Sigma_\xi, \Sigma_A, \Sigma_\psi, \Sigma_B)$ if

$$\mu(t) = \Theta \xi(t) \psi(t) \tag{1a}$$

$$\Sigma(t) = \Theta \xi(t) \xi(t)^T \Theta^T + \Sigma_0 \tag{1b}$$

155 where Θ is a $p \times L$ matrix of constant coefficients, $\Sigma_0 = \text{diag}(\sigma_1^2, \dots, \sigma_p^2)$, while $\xi(t)_{L \times K}$ and
 156 $\psi(t)_{K \times 1}$ are matrices comprising continuous dictionary functions evolving in time through
 157 nGP, $\xi_{lk}(t) \sim \text{nGP}([\Sigma_\xi]_{lk} = \sigma_{\xi_{lk}}^2, [\Sigma_A]_{lk} = \sigma_{A_{lk}}^2)$ and $\psi_k(t) \sim \text{nGP}([\Sigma_\psi]_k = \sigma_{\psi_k}^2, [\Sigma_B]_k =$
 158 $\sigma_{B_k}^2)$.

159 Restricting our attention on the generic element $\xi_{lk}(t) : \mathcal{T} \rightarrow \mathfrak{R}$ of the matrix $\xi(t)_{L \times K}$
 160 (the same holds for $\psi_k(t) : \mathcal{T} \rightarrow \mathfrak{R}$), the nGP provides a highly flexible stochastic process on
 161 the dictionary functions whose smoothness, explicitly modeled by their m th order deriva-
 162 tives $D^m \xi_{lk}(t)$ via stochastic differential equations (SDEs), is expected to be centered on a
 163 local instantaneous mean function $A_{lk}(t)$, which represents a higher-level Gaussian Process
 164 (GP), that induces adaptivity to locally-varying smoothing. Specifically, we let

$$D^m \xi_{lk}(t) = A_{lk}(t) + \sigma_{\xi_{lk}} W_{\xi_{lk}}(t), \quad m \in N, \quad m \geq 2, \tag{2a}$$

$$D^n A_{lk}(t) = \sigma_{A_{lk}} W_{A_{lk}}(t), \quad n \in N, \quad n \geq 1, \tag{2b}$$

165 where $\sigma_{\xi_{lk}} \in \mathfrak{R}^+$, $\sigma_{A_{lk}} \in \mathfrak{R}^+$, $W_{\xi_{lk}}(t) : \mathcal{T} \rightarrow \mathfrak{R}$ and $W_{A_{lk}}(t) : \mathcal{T} \rightarrow \mathfrak{R}$ are independent
 166 Gaussian white noise processes with mean $E[W_{\xi_{lk}}(t)] = E[W_{A_{lk}}(t)] = 0$, for all $t \in \mathcal{T}$, and
 167 covariance function $E[W_{\xi_{lk}}(t)W_{\xi_{lk}}(t')] = E[W_{A_{lk}}(t)W_{A_{lk}}(t')] = 1$ if $t = t'$, 0 otherwise. This
 168 formulation naturally induces a stochastic process for $\xi_{lk}(t)$ with varying smoothness, where
 169 $E[D^m \xi_{lk}(t)|A_{lk}(t)] = A_{lk}(t)$, and initialization at t_1 based on the assumption

$$\begin{aligned} [\xi_{lk}(t_1), D^1 \xi_{lk}(t_1), \dots, D^{m-1} \xi_{lk}(t_1)]^T &\sim N_m(0, \sigma_{\mu_{lk}}^2 I_m) \\ [A_{lk}(t_1), D^1 A_{lk}(t_1), \dots, D^{n-1} A_{lk}(t_1)]^T &\sim N_n(0, \sigma_{\alpha_{lk}}^2 I_n) \end{aligned}$$

170 The Markovian property implied by SDEs in (2a) and (2b) represents a key advantage
 171 in terms of computational tractability as it allows a simple state space formulation. In
 172 particular, referring to Zhu and Dunson (2012) for $m = 2$ and $n = 1$ (this can be easily
 173 extended for higher m and n), and for $\delta_i = t_{i+1} - t_i$ sufficiently small, the process for $\xi_{lk}(t)$
 174 along with its first order derivative $\xi'_{lk}(t)$ and the local instantaneous mean $A_{lk}(t)$ follow
 175 the approximated state equation

$$\begin{bmatrix} \xi_{lk}(t_{i+1}) \\ \xi'_{lk}(t_{i+1}) \\ A_{lk}(t_{i+1}) \end{bmatrix} = \begin{bmatrix} 1 & \delta_i & 0 \\ 0 & 1 & \delta_i \\ 0 & 0 & 1 \end{bmatrix} \begin{bmatrix} \xi_{lk}(t_i) \\ \xi'_{lk}(t_i) \\ A_{lk}(t_i) \end{bmatrix} + \begin{bmatrix} 0 & 0 \\ 1 & 0 \\ 0 & 1 \end{bmatrix} \begin{bmatrix} \omega_{i,\xi_{lk}} \\ \omega_{i,A_{lk}} \end{bmatrix}, \quad (3)$$

176 where $[\omega_{i,\xi_{lk}}, \omega_{i,A_{lk}}]^T \sim N_2(0, V_{i,lk})$, with $V_{i,lk} = \text{diag}(\sigma_{\xi_{lk}}^2 \delta_i, \sigma_{A_{lk}}^2 \delta_i)$.

177 Similarly to the nGP specification for the elements in $\xi(t)$, we can represent the nested
 178 Gaussian Process for $\psi_k(t)$ with the following state equation

$$\begin{bmatrix} \psi_k(t_{i+1}) \\ \psi'_k(t_{i+1}) \\ B_k(t_{i+1}) \end{bmatrix} = \begin{bmatrix} 1 & \delta_i & 0 \\ 0 & 1 & \delta_i \\ 0 & 0 & 1 \end{bmatrix} \begin{bmatrix} \psi_k(t_i) \\ \psi'_k(t_i) \\ B_k(t_i) \end{bmatrix} + \begin{bmatrix} 0 & 0 \\ 1 & 0 \\ 0 & 1 \end{bmatrix} \begin{bmatrix} \omega_{i,\psi_k} \\ \omega_{i,B_k} \end{bmatrix} \quad (4)$$

179 independently for $k = 1, \dots, K$, where $[\omega_{i,\psi_k}, \omega_{i,B_k}]^T \sim N_2(0, S_{i,k})$, with $S_{i,k} = \text{diag}(\sigma_{\psi_k}^2 \delta_i, \sigma_{B_k}^2 \delta_i)$.

180 Similarly to $\xi_{lk}(t)$

$$\begin{aligned} [\psi_k(t_1), D^1 \psi_k(t_1), \dots, D^{m-1} \psi_k(t_1)]^T &\sim N_m(0, \sigma_{\mu_k}^2 I_m), \\ [B_k(t_1), D^1 B_k(t_1), \dots, D^{n-1} B_k(t_1)]^T &\sim N_n(0, \sigma_{\alpha_k}^2 I_n), \end{aligned}$$

181 There are two crucial aspects to highlight. Firstly, this formulation allows continuous time
 182 and an irregular grid of observations over t by relating the latent states at $i + 1$ to those
 183 at i through the distance between t_{i+1} and t_i where i represents a discrete order index
 184 and $t_i \in \mathcal{T}$ the time value related to the i th observation. Secondly, compared to Zhu
 185 and Dunson (2012) our approach represents an important generalization in: (i) extending
 186 the analysis to the multivariate case (i.e. y_i is a p -dimensional vector instead of a scalar)
 187 and (ii) accommodating locally adaptive smoothing not only on the mean but also on the
 188 time-varying covariance functions.

189 2.3 LAF interpretation

190 Model (1a)-(1b) can be induced by marginalizing out the K -dimensional latent factors
 191 vector η_i , in the model

$$Y_i = \Lambda(t_i)\eta_i + \epsilon_i, \quad \epsilon_i \sim N_p(0, \Sigma_0) \quad (5)$$

192 where $\eta_i = \psi(t_i) + \nu_i$ with $\nu_i \sim N_K(0, I_K)$ and elements $\psi_k(t) \sim \text{nGP}(\sigma_{\psi_k}^2, \sigma_{B_k}^2)$ for $k =$
 193 $1, \dots, K$. In LAF formulation we assume moreover that the time-varying factor loadings
 194 matrix $\Lambda(t)$ is a sparse linear combination, with respect to the weights of the $p \times L$ matrix
 195 Θ , of a much smaller set of continuous nested Gaussian Processes $\xi_{lk}(t) \sim \text{nGP}(\sigma_{\xi_{lk}}^2, \sigma_{A_{lk}}^2)$
 196 comprising the $L \times K$, with $L \ll p$, matrix $\xi(t)$. As a result

$$\Lambda(t_i) = \Theta \xi(t_i) \tag{6}$$

Such a decomposition plays a crucial role in further reducing the number of nGP processes to be modeled from $p \times K$ to $L \times K$ leading to a more computationally tractable formulation in which the induced $\Gamma = \{\mu(t), \Sigma(t), t \in \mathcal{T}\}$ follows a locally adaptive factor LAF $_{L,K}(\Theta, \Sigma_0, \Sigma_\xi, \Sigma_A, \Sigma_\psi, \Sigma_B)$ process where

$$\mu(t_i) = E(Y_i | t = t_i) = \Theta \xi(t_i) \psi(t_i) \tag{7a}$$

$$\Sigma(t_i) = \text{cov}(Y_i | t = t_i) = \Theta \xi(t_i) \xi(t_i)^T \Theta^T + \Sigma_0. \tag{7b}$$

197 There is a literature on using Bayesian factor analysis with time-varying loadings, but
 198 essentially all the literature assumes discrete-time dynamics on the loadings while our focus
 199 is instead on allowing the loadings, and hence the induced $\Gamma = \{\mu(t), \Sigma(t), t \in \mathcal{T}\}$ processes,
 200 to evolve flexibly in continuous time. Hence, we are most closely related to the literature on
 201 Gaussian process latent factor models for spatial and temporal data; refer, for example, to
 202 Lopes, Salazar and Gamerman (2008) and Lopes, Gamerman and Salazar (2011). In these
 203 models, the factor loadings matrix characterizes spatial dependence, with time varying
 204 factors accounting for dynamic changes.

205 Fox and Dunson (2011) instead allow the loadings matrix to vary through a continuous
 206 time stochastic process built from latent GP(0, c) dictionary functions independently for all
 207 l, k , with c the squared exponential correlation function having $c(x, x') = \exp(-\kappa \|x - x'\|_2^2)$.
 208 In our work we follow the lead of Fox and Dunson (2011) in using a nonparametric latent factor
 209 model as in (5)-(6), but induce fundamentally different behavior on $\Gamma = \{\mu(t), \Sigma(t), t \in$
 210 $\mathcal{T}\}$ by carefully modifying the stochastic processes for the dictionary functions.

211 Note that the above decomposition of $\Gamma = \{\mu(t), \Sigma(t), t \in \mathcal{T}\}$ is not unique. Potentially
 212 we could constrain the loadings matrix to enforce identifiability (Geweke and Zhou, 1996),
 213 but this approach induces an undesirable order dependence among the responses (Aguilar
 214 and West, 2000, West, 2003, Lopes and West, 2004, Carvalho et al., 2008). Given our
 215 focus on estimation of Γ we follow Ghosh and Dunson (2009) in avoiding identifiability
 216 constraints, as such constraints are not necessary to ensure identifiability of the induced
 217 mean $\mu(t)$ and covariance $\Sigma(t)$. The characterization of the class of time-varying covariance
 218 matrices $\Sigma(t)$ is proved by Lemma 2.1 of Fox and Dunson (2011) which states that for K
 219 and L sufficiently large, any covariance regression can be decomposed as in (1b). Similar
 220 results are obtained for the mean process.

221 2.4 Prior Specification

222 We adopt a hierarchical prior specification approach to induce a prior P on $\Gamma = \{\mu(t), \Sigma(t), t \in$
 223 $\mathcal{T}\}$ with the goal of maintaining simple computation and allowing both covariances and
 224 means to evolve flexibly over continuous time. Specifically

- 225 • $\Gamma|\Theta, \Sigma_0, \Sigma_\xi, \Sigma_A, \Sigma_\psi, \Sigma_B \sim \text{LAF}_{L,K}(\Theta, \Sigma_0, \Sigma_\xi, \Sigma_A, \Sigma_\psi, \Sigma_B)$
 226 • Recalling the nGP assumption for the elements of $\xi(t)_{L \times K}$: $\xi_{lk}(t) \sim \text{nGP}(\sigma_{\xi_{lk}}^2, \sigma_{A_{lk}}^2)$
 227 within LAF representation, we assume for each element $[\Sigma_\xi]_{lk}$ and $[\Sigma_A]_{lk}$ of the
 228 $L \times K$ matrices Σ_ξ and Σ_A respectively, the following priors

$$\begin{aligned} \sigma_{\xi_{lk}}^2 &\sim \text{InvGa}(a_\xi, b_\xi) \\ \sigma_{A_{lk}}^2 &\sim \text{InvGa}(a_A, b_A) \end{aligned}$$

229 independently for each (l, k) ; where $\text{InvGa}(a, b)$ denotes the Inverse Gamma distribu-
 230 tion with shape a and scale b .

- 231 • Similarly, the variances $[\Sigma_\psi]_k = \sigma_{\psi_k}^2$ and $[\Sigma_B]_k = \sigma_{B_k}^2$ in the state equation represen-
 232 tation of the nGP for each $\psi_k(t) \sim \text{nGP}(\sigma_{\psi_k}^2, \sigma_{B_k}^2)$ are assumed

$$\begin{aligned} \sigma_{\psi_k}^2 &\sim \text{InvGa}(a_\psi, b_\psi) \\ \sigma_{B_k}^2 &\sim \text{InvGa}(a_B, b_B) \end{aligned}$$

233 independently for each k .

- 234 • To address the issue related to the selection of the number of dictionary elements a
 235 shrinkage prior is proposed for Θ . In particular, following Bhattacharya and Dunson
 236 (2011) we assume:

$$\begin{aligned} \theta_{jl}|\phi_{jl}, \tau_l &\sim \text{N}(0, \phi_{jl}^{-1} \tau_l^{-1}) \quad \phi_{jl} \sim \text{Ga}(3/2, 3/2) \\ \vartheta_1 &\sim \text{Ga}(a_1, 1), \quad \vartheta_h \sim \text{Ga}(a_2, 1), h \geq 2, \quad \tau_l = \prod_{h=1}^l \vartheta_h \end{aligned} \quad (8)$$

237 Note that if $a_2 > 1$ the expected value for ϑ_h is greater than 1. As a result, as l goes
 238 to infinity, τ_l tends to infinity shrinking θ_{jl} towards zero. This leads to a flexible prior
 239 for θ_{jl} with a local shrinkage parameter ϕ_{jl} and a global column-wise shrinkage factor
 240 τ_l which allows many elements of Θ being close to zero as L increases.

- 241 • Finally for the variances of the error terms in vector ϵ_i , we assume the usual inverse
 242 gamma prior distribution. Specifically

$$\sigma_j^{-2} \sim \text{Ga}(a_\sigma, b_\sigma)$$

243 independently for each $j = 1, \dots, p$.

244 3. Posterior Computation

245 For a fixed truncation level L^* and a latent factor dimension K^* , the algorithm for posterior
 246 computation alternates between a simple and efficient simulation smoother step (Durbin
 247 and Koopman, 2002) to update the state space formulation of the nGP in LAF prior, and
 248 standard Gibbs sampling steps for updating the parametric component parameters from
 249 their full conditional distributions.

250 **3.1 Gibbs Sampling**

251 We outline here the main features of the algorithm for posterior computation based on ob-
 252 servations (y_i, t_i) for $i = 1, \dots, T$, while the complete algorithm is provided in the Appendix.

253 A. Given Θ and $\{\eta_i\}_{i=1}^T$, a multivariate version of the MCMC algorithm proposed by Zhu
 254 and Dunson (2012) draws posterior samples from each dictionary element's function
 255 $\{\xi_{lk}(t_i)\}_{i=1}^T$, its first order derivative $\{\xi'_{lk}(t_i)\}_{i=1}^T$, the corresponding instantaneous
 256 mean $\{A_{lk}(t_i)\}_{i=1}^T$, the variances in the state equations $\sigma_{\xi_{lk}}^2, \sigma_{A_{lk}}^2$ and the variances of
 257 the error terms in the observation equation σ_j^2 with $j = 1, \dots, p$.

258 B. Given $\Theta, \{\sigma_j^{-2}\}_{j=1}^p, \{y_i\}_{i=1}^T$ and $\{\xi(t_i)\}_{i=1}^T$ we implement a block sampling of $\{\psi(t_i)\}_{i=1}^T,$
 259 $\{\psi'_k(t_i)\}_{i=1}^T, \{B_k(t_i)\}_{i=1}^T, \sigma_{\psi_k}^2, \sigma_{B_k}^2$ and ν_i following a similar approach as in step A.

260 C. Conditioned on $\{y_i\}_{i=1}^T, \{\eta_i\}_{i=1}^T, \{\sigma_j^{-2}\}_{j=1}^p$ and $\{\xi(t_i)\}_{i=1}^T$, and recalling the shrinkage
 261 prior for the elements of Θ in (8), we update Θ , each local shrinkage hyperparameter
 262 ϕ_{jl} and the global shrinkage hyperparameters τ_l following the standard conjugate
 263 analysis.

264 D. Given the posterior samples from $\Theta, \Sigma_0, \{\xi(t_i)\}_{i=1}^T$ and $\{\psi(t_i)\}_{i=1}^T$ the realization of
 265 LAF process for $\{\mu(t_i), \Sigma(t_i), t_i \in \mathcal{T}\}$ conditioned on the data $\{y_i\}_{i=1}^T$ is

$$\begin{aligned} \mu(t_i) &= \Theta \xi(t_i) \psi(t_i) \\ \Sigma(t_i) &= \Theta \xi(t_i) \xi(t_i)^T \Theta^T + \Sigma_0. \end{aligned}$$

266 **3.2 Hyperparameter interpretation**

267 We now focus our attention on the hyperparameters of the priors for $\sigma_{\xi_{lk}}^2, \sigma_{A_{lk}}^2, \sigma_{\psi_k}^2$ and
 268 $\sigma_{B_k}^2$. Several simulation studies have shown that the higher the variances in the latent state
 269 equations, the better our formulation accommodates locally adaptive smoothing for sudden
 270 changes in Γ . A theoretical support for this data-driven consideration can be identified
 271 in the connection between the nGP and the nested smoothing splines. It has been shown
 272 by Zhu and Dunson (2012) that the posterior mean of the trajectory U with reference to
 273 the problem of nonparametric mean regression under the nGP prior can be related to the
 274 minimizer of the equation

$$\frac{1}{T} \sum_{i=1}^T (y_i - U(t_i))^2 + \lambda_U \int_{\mathcal{T}} (D^m U(t) - C(t))^2 dt + \lambda_C \int_{\mathcal{T}} (D^n C(t))^2 dt,$$

275 where C is the locally instantaneous function and $\lambda_U \in \mathbb{R}^+$ and $\lambda_C \in \mathbb{R}^+$ regulate the
 276 smoothness of the unknown functions U and C respectively, leading to less smoothed pat-
 277 terns when fixed at low values. The resulting inverse relationship between these smoothing
 278 parameters and the variances in the state equation, together with the results in the simula-
 279 tion studies, suggest to fix the hyperparameters in the Inverse Gamma prior for $\sigma_{\xi_{lk}}^2, \sigma_{A_{lk}}^2,$
 280 $\sigma_{\psi_k}^2$ and $\sigma_{B_k}^2$ so as to allow high variances in the case in which the time series analyzed are
 281 expected to have strong changes in their covariance (or mean) dynamic. A further confir-
 282 mation of the previous discussion is provided by the structure of the simulation smoother

283 required to update the dictionary functions in our Gibbs Sampling for posterior computa-
 284 tion. More specifically, the larger the variances of $\{\omega_{i,\xi_{lk}}\}_{i=1}^T$, $\{\omega_{i,A_{lk}}\}_{i=1}^T$ and $\{\omega_{i,\psi_k}\}_{i=1}^T$,
 285 $\{\omega_{i,B_k}\}_{i=1}^T$ in the state equations, with respect to those of the vector of observations $\{y_i\}_{i=1}^T$,
 286 the higher is the weight associated to innovations in the filtering and smoothing techniques,
 287 allowing for less smoothed patterns both in the covariance and mean structures (see Durbin
 288 and Koopman, 2002).

289 In practical applications, it may be useful to obtain a first estimate of $\tilde{\Gamma} = \{\tilde{\mu}(t), \tilde{\Sigma}(t)\}$ to
 290 set the hyperparameters. More specifically, $\tilde{\mu}_j(t_i)$ can be the output of a standard moving
 291 average on each time series $y_j = [y_{j1}, \dots, y_{jT}]$, while $\tilde{\Sigma}(t_i)$ can be obtained by a simple
 292 estimator, such as the EWMA procedure. With these choices, the recursive equation

$$\tilde{\Sigma}(t_i) = (1 - \lambda)\{[y_{i-1} - \tilde{\mu}(t_{i-1})][y_{i-1} - \tilde{\mu}(t_{i-1})]^T\} + \lambda\tilde{\Sigma}(t_{i-1})$$

293 become easy to implement.

294 3.3 Online Updating

295 The problem of online updating represents a key point in multivariate time series with high
 296 frequency data. Referring to our formulation, we are interested in updating an approximated
 297 posterior distribution for $\Gamma_{T+H} = \{\mu(t_{T+h}), \Sigma(t_{T+h}), h = 1, \dots, H\}$ once a new vector of
 298 observations $\{y_i\}_{i=T+1}^{T+H}$ is available, instead of rerunning posterior computation for the whole
 299 time series.

300 Using the posterior estimates of the Gibbs sampler based on observations available up
 301 to time T , $\{y_i\}_{i=1}^T$, it is easy to implement (see in Appendix) a highly computationally
 302 tractable online updating algorithm which alternates between steps A, B and D outlined in
 303 the previous section for the new set of observations, and that can be initialized at $T + 1$
 304 using the one step ahead predictive distribution for the latent state vectors in the state
 305 space formulation.

306 Note that the initialization procedure for latent state vectors in the algorithm depends on
 307 the sample moments of the posterior distribution for the latent states at T . As is known for
 308 Kalman smoothers (see, e.g., Durbin and Koopman, 2001), this could lead to computational
 309 problems in the online updating due to the larger conditional variances of the latent states
 310 at the end of the sample (i.e., at T). To overcome this problem, we replace the previous
 311 assumptions for the initial values with a data-driven initialization scheme. In particular,
 312 instead of using only the new observations for the online updating, we run the algorithm
 313 for $\{y_i\}_{i=T-k}^{T+H}$, with k small, and choosing a diffuse but proper prior for the initial states at
 314 $T - k$. As a result the distribution of the smoothed states at T is not anymore affected by
 315 the problem of large conditional variances leading to better online updating performance.

316 4. Simulation Studies

317 The aim of the following simulation studies is to compare the performance of our pro-
 318 posed LAF with respect to BCR, and to the models for multivariate stochastic volatility
 319 most widely used in practice, specifically: EWMA, PC-GARCH, GO-GARCH and DCC-
 320 GARCH. In order to assess whether and to what extent LAF can accommodate, in practice,
 321 even sharp changes in the time-varying means and covariances and to evaluate the costs of

322 our flexible approach in settings where the mean and covariance functions do not require
 323 locally adaptive estimation techniques, we focus on two different sets of simulated data.
 324 The first is based on an underlying structure characterized by locally varying smoothness
 325 processes, while the second has means and covariances evolving in time through smooth
 326 processes. In the last subsection we also analyze the performance of the proposed online
 327 updating algorithm.

328 4.1 Simulated Data

329 A. Locally varying smoothness processes: We generate a set of 5-dimensional observations
 330 y_i for each t_i in the discrete set $\mathcal{T}_o = \{1, 2, \dots, 100\}$, from the latent factor model
 331 in (5) with $\Lambda(t_i) = \Theta\xi(t_i)$. To allow sharp changes of means and covariances in
 332 the generating mechanism, we consider a 2×2 (i.e. $L = K = 2$) matrix $\{\xi(t_i)\}_{i=1}^{100}$
 333 of time-varying functions adapted from Donoho and Johnstone (1994) with locally-
 334 varying smoothness (more specifically we choose ‘bumps’ functions). The latent mean
 335 dictionary elements $\{\psi(t_i)\}_{i=1}^{100}$ are simulated from a Gaussian process $\text{GP}(0, c)$ with
 336 length scale $\kappa = 10$, while the elements in matrix Θ can be obtained from the shrinkage
 337 prior in (8) with $a_1 = a_2 = 10$. Finally the elements of the diagonal matrix Σ_0^{-1} are
 338 sampled independently from $\text{Ga}(1, 0.1)$.

339 B. Smooth processes: We consider the same dataset of 10-dimensional observations y_i
 340 with $t_i \in \mathcal{T}_o = \{1, 2, \dots, 100\}$ investigated in Fox and Dunson (2011, section 4.1). The
 341 settings are similar to the previous with exception of $\{\xi(t_i)\}_{i=1}^{100}$ which are 5×4 (i.e.
 342 $L = 5, K = 4$) matrices of smooth GP dictionary functions with length-scale $\kappa = 10$.

343 4.2 Estimation Performance

344 A. Locally varying smoothness processes:
 345 Posterior computation for LAF is performed by using truncation levels $L^* = K^* = 2$
 346 (at higher level settings we found that the shrinkage prior on Θ results in posterior
 347 samples of the elements in the additional columns concentrated around 0). We place a
 348 $\text{Ga}(1, 0.1)$ prior on the precision parameters σ_j^{-2} and choose $a_1 = a_2 = 2$. As regards
 349 the nGP prior for each dictionary element $\xi_{lk}(t)$ with $l = 1, \dots, L^*$ and $k = 1, \dots, K^*$,
 350 we choose diffuse but proper priors for the initial values by setting $\sigma_{\mu_{lk}}^2 = \sigma_{\alpha_{lk}}^2 = 100$
 351 and place an $\text{InvGa}(2, 10^8)$ prior on each $\sigma_{\xi_{lk}}^2$ and $\sigma_{A_{lk}}^2$ in order to allow less smoothed
 352 behavior according to a previous graphical analysis of $\tilde{\Sigma}(t_i)$ estimated via EWMA.
 353 Similarly we set $\sigma_{\mu_k}^2 = \sigma_{\alpha_k}^2 = 100$ in the prior for the initial values of the latent state
 354 equations resulting from the nGP prior for $\psi_k(t)$, and consider $a_\psi = a_B = b_\psi = b_B =$
 355 0.005 to balance the rough behavior induced on the nonparametric mean functions by
 356 the settings of the nGP prior on $\xi_{lk}(t)$, as suggested from previous graphical analysis.
 357 Note also that for posterior computation, we first scale the predictor space to $(0, 1]$,
 358 leading to $\delta_i = 1/100$, for $i = 1, \dots, 100$.

359 For inference in BCR we consider the same previous hyperparameters setting for Θ
 360 and Σ_0 priors as well as the same truncation levels K^* and L^* , while the length scale
 361 κ in GP prior for $\xi_{lk}(t)$ and $\psi_k(t)$ has been set to 10 using the data-driven heuristic

362 outlined in Fox and Dunson (2011). In both cases we run 50,000 Gibbs iterations
 363 discarding the first 20,000 as burn-in and thinning the chain every 5 samples.

364 As regards the other approaches, EWMA has been implemented by choosing the
 365 smoothing parameter λ that minimizes the mean squared error (MSE) between the
 366 estimated covariances and the true values. PC-GARCH algorithm follows the steps
 367 provided by Burns (2005) with GARCH(1,1) assumed for the conditional volatilities
 368 of each single time series and the principal components. GO-GARCH and DCC-
 369 GARCH recall the formulations provided by van der Wiede (2002) and Engle (2002)
 370 respectively, assuming a GARCH(1,1) for the conditional variances of the processes
 371 analyzed, which proves to be a correct choice in many financial applications and also in
 372 our setting. Note that, differently from LAF and BCR, the previous approaches do not
 373 model explicitly the mean process $\{\mu(t_i)\}_{i=1}^{100}$ but work directly on the innovations $\{y_i -$
 374 $\mu(t_i)\}_{i=1}^{100}$. Therefore in these cases we first model the conditional mean via smoothing
 375 spline and in a second step we estimate the models working on the innovations. The
 376 smoothing parameter for spline estimation has been set to 0.7, which was found to be
 377 appropriate to best reproduce the true dynamic of $\{\mu(t_i)\}_{i=1}^{100}$.

378 B. Smooth processes:

379 We mainly keep the same setting of the previous simulation study with few differences.
 380 Specifically, L^* and K^* has been fixed to 5 and 4 respectively (also in this case the
 381 choice of the truncation levels proves to be appropriate, reproducing the same results
 382 provided in the simulation study of Fox and Dunson (2011) where $L^* = 10$ and
 383 $K^* = 10$). Moreover the scale parameters in the Inverse Gamma prior on each $\sigma_{\xi_{lk}}^2$
 384 and $\sigma_{A_{lk}}^2$ has been set to 10^4 in order to allow a smoother behavior according to a
 385 previous graphical analysis of $\tilde{\Sigma}(t_i)$ estimated via EWMA, but without forcing the
 386 nGP prior to be the same as a GP prior. Following Fox and Dunson (2011) we
 387 run 10,000 Gibbs iterations which proved to be enough to reach convergence, and
 388 discarded the first 5,000 as burn-in.

389 In the first set of simulated data, we analyzed mixing by the Gelman-Rubin procedure (see
 390 e.g. Gelman and Rubin, 1992), based on potential scale reduction factors computed for each
 391 chain by splitting the sampled quantities in 6 pieces of same length. The analysis shows
 392 slower mixing for BCR compared with LAF. Specifically, in LAF 95% of the chains have a
 393 potential reduction factor lower than 1.35, with a median equal to 1.11, while in BCR the
 394 95th quantile is 1.44 and the median equals 1.18. Less problematic is the mixing for the
 395 second set of simulated data, with potential scale reduction factors having median equal
 396 to 1.05 for both approaches and 95th quantiles equal to 1.15 and 1.31 for LAF and BCR,
 397 respectively.

398 Figure 2 compares, in both simulated samples, true and posterior mean of the process
 399 $\Gamma = \{\mu(t_i), \Sigma(t_i), i = 1, \dots, 100\}$ over the predictor space \mathcal{T}_o together with the point-wise
 400 95% highest posterior density (hpd) intervals for LAF and BCR. From the upper plots
 401 we can clearly note that our approach is able to capture conditional heteroscedasticity as
 402 well as mean patterns, also in correspondence of sharp changes in the time-varying true
 403 functions. The major differences compared to the true values can be found at the beginning
 404 and at the end of the series and are likely to be related to the structure of the simulation

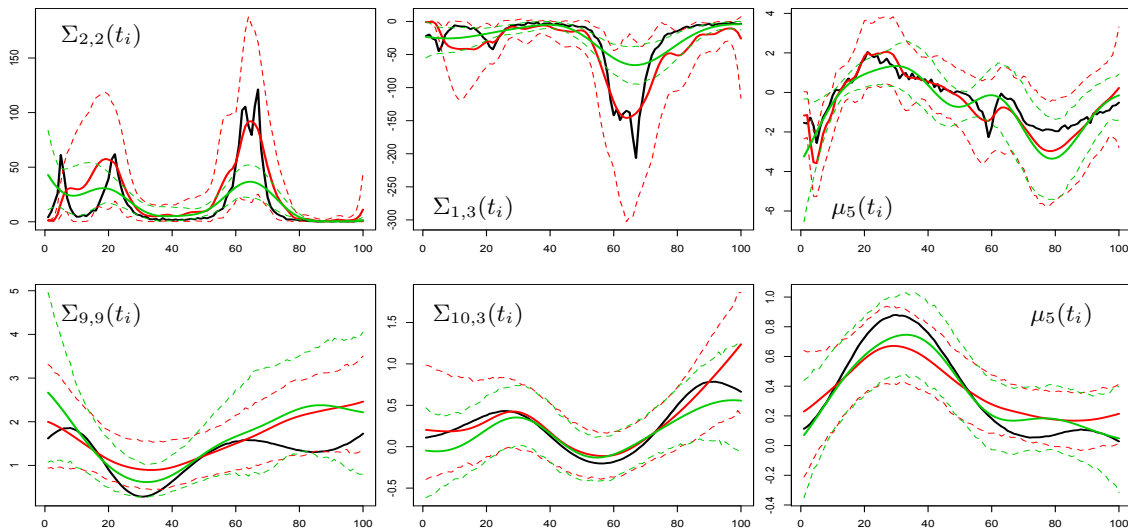


Figure 2: For locally varying smoothness simulation (top) and smooth simulation (bottom), plots of truth (black) and posterior mean respectively of LAF (solid red line) and BCR (solid green line) for selected components of the variance (left), covariance (middle), mean (right). For both approaches the dotted lines represent the 95% highest posterior density intervals.

405 smoother which also causes a widening of the credibility bands at the very end of the series;
 406 for references regarding this issue see Durbin and Koopman (2001). However, even in the
 407 most problematic cases, the true values are within the bands of the 95% hpd intervals.
 408 Much more problematic is the behavior of the posterior distributions for BCR which badly
 409 over-smooth both covariance and mean functions leading also to many 95% hpd intervals
 410 not containing the true values. Bottom plots in Figure 2 show that the performance of our
 411 approach is very close to that of BCR, when data are simulated from a model where the
 412 covariances and means evolve smoothly across time and local adaptivity is therefore not
 413 required. This happens even if the hyperparameters in LAF are set in order to maintain
 414 separation between nGP and GP prior, suggesting large support property for the proposed
 415 approach.

416 The comparison of the summaries of the squared errors between true process $\Gamma =$
 417 $\{\mu(t_i), \Sigma(t_i), i = 1, \dots, 100\}$ and the estimated elements of $\hat{\Gamma} = \{\hat{\mu}(t_i), \hat{\Sigma}(t_i), i = 1, \dots, 100\}$
 418 standardized with the range of the true processes $r_\mu = \max_{i,j} \{\mu_k(t_i)\} - \min_{i,j} \{\mu_j(t_i)\}$ and
 419 $r_\Sigma = \max_{i,j,k} \{\Sigma_{j,k}(t_i)\} - \min_{i,j,k} \{\Sigma_{j,k}(t_i)\}$ respectively, once again confirms the overall bet-
 420 ter performance of our approach relative to all the considered competitors. Table 1 shows
 421 that, when local adaptivity is required, LAF provides a superior performance having stan-
 422 dardized residuals lower than those of the other approaches. EWMA seems to provide quite
 423 accurate estimates, but it is important to underline that we choose the optimal smoothing
 424 parameter λ in order to minimize the MSE between estimated and true parameters, which
 425 are clearly not known in practical applications. Different values of λ reduces significantly
 426 the performance of EWMA, which shows also lack of robustness. The closeness of the sum-
 427 maries of LAF and BCR in Table 2 confirms the flexibility of LAF even in settings where

	Mean	90th Quantile	95th Quantile	Max
	Covariance $\{\Sigma(t_i)\}$			
EWMA	1.37	2.28	5.49	85.86
PC-GARCH	1.75	2.49	6.48	229.50
GO-GARCH	2.40	3.66	10.32	173.41
DCC-GARCH	1.75	2.21	6.95	226.47
BCR	1.80	2.25	7.32	142.26
LAF	0.90	1.99	4.52	36.95
	Mean $\{\mu(t_i)\}$			
SPLINE	0.064	0.128	0.186	2.595
BCR	0.087	0.185	0.379	2.845
LAF	0.062	0.123	0.224	2.529

Table 1: LOCALLY VARYING SMOOTHNESS PROCESSES: Summaries of the standardized squared errors between true values $\{\mu(t_i)\}_{i=1}^{100}$ and $\{\Sigma(t_i)\}_{i=1}^{100}$ and estimated quantities $\{\hat{\Sigma}(t_i)\}_{i=1}^{100}$ and $\{\hat{\mu}(t_i)\}_{i=1}^{100}$ computed with different approaches.

	Mean	90th Quantile	95th Quantile	Max
	Covariance $\{\Sigma(t_i)\}$			
EWMA	0.030	0.081	0.133	1.119
PC-GARCH	0.018	0.048	0.076	0.652
GO-GARCH	0.043	0.104	0.202	1.192
DCC-GARCH	0.022	0.057	0.110	0.466
BCR	0.009	0.019	0.039	0.311
LAF	0.009	0.022	0.044	0.474
	Mean $\{\mu(t_i)\}$			
SPLINE	0.007	0.019	0.027	0.077
BCR	0.005	0.015	0.024	0.038
LAF	0.005	0.017	0.026	0.050

Table 2: SMOOTH PROCESSES: Summaries of the standardized squared errors between true values $\{\mu(t_i)\}_{i=1}^{100}$ and $\{\Sigma(t_i)\}_{i=1}^{100}$ and estimated quantities $\{\hat{\Sigma}(t_i)\}_{i=1}^{100}$ and $\{\hat{\mu}(t_i)\}_{i=1}^{100}$ computed with different approaches.

428 local adaptivity is not required and highlights the better performance of the two approaches
 429 with respect to the other competitors also when smooth processes are investigated.

430 To better understand the improvement of our approach in allowing locally varying
 431 smoothness and to evaluate the consequences of the over-smoothing induced by BCR on the
 432 distribution of y_i with $i = 1, \dots, 100$ consider Figure 3 which shows, for some selected series
 433 $\{y_{ji}\}_{i=1}^{100}$ in the first simulated dataset, the time varying mean together with the point-wise
 434 2.5% and 97.5% quantiles of the marginal distribution of y_{ji} induced respectively by the
 435 true mean and true variance, the posterior mean of $\mu_j(t_i)$ and $\Sigma_{jj}(t_i)$ from our proposed
 436 approach and the posterior mean of the same quantities from BCR. We can clearly see
 437 that the marginal distribution of y_{ji} induced by BCR is over-concentrated near the mean,
 438 leading to incorrect inferences. Note that our proposal is also able to accommodate heavy
 439 tails, a typical characteristic in financial series.

440 4.3 Online Updating Performance

441 To analyze the performance of the online updating algorithm in LAF model, we simulate
 442 50 new observations $\{y_i\}_{i=101}^{150}$ with $t_i \in \mathcal{T}_o^* = \{101, \dots, 150\}$, considering the same Θ and

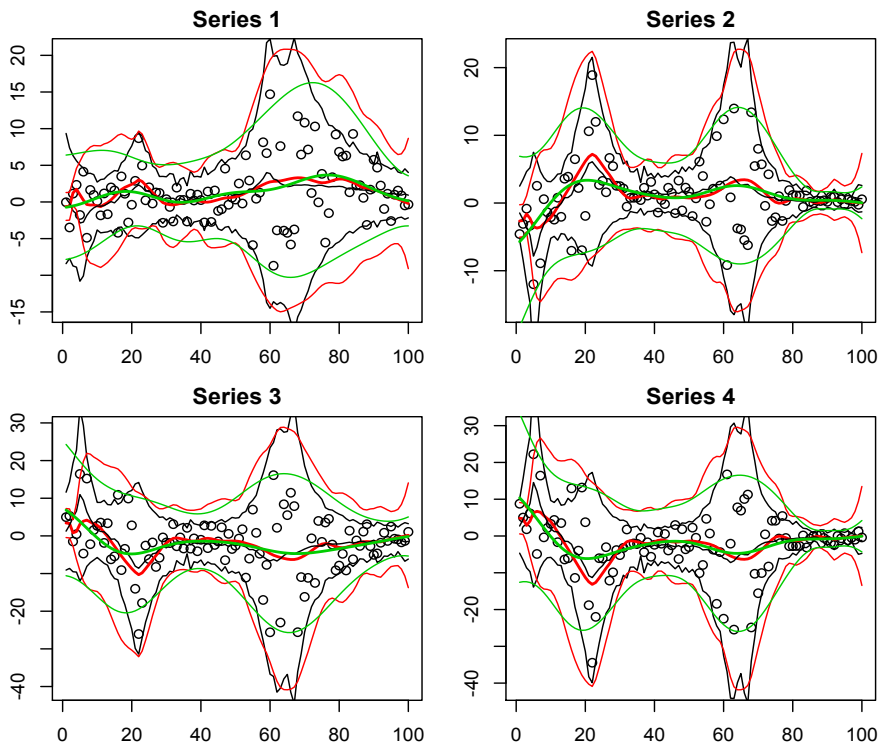


Figure 3: Plot for 4 selected simulated series of the time-varying mean $\mu_j(t_i)$ and the time-varying 2.5% and 97.5% quantiles of the marginal distribution of y_{ji} with true mean and variance (black), mean and variance from posterior mean of LAF (red), mean and variance from posterior mean of BCR (green). Black points represent the simulated data.

443 Σ_0 used in the generating mechanism for the first simulated dataset and taking the 50
 444 subsequent observations of the bumps functions for the dictionary elements $\{\xi(t_i)\}_{i=101}^{150}$;
 445 finally the additional latent mean dictionary elements $\{\psi(t_i)\}_{i=101}^{150}$ are simulated as before
 446 maintaining the continuity with the previously simulated functions $\{\psi(t_i)\}_{i=1}^{100}$. According to
 447 the algorithm described in subsection 3.3, we fix Θ , Σ_0 , Σ_ξ , Σ_A , Σ_ψ and Σ_B at their posterior
 448 mean from the previous Gibbs sampler and consider the last three observations y_{98} , y_{99} and
 449 y_{100} (i.e. $k = 3$) to initialize the simulation smoother in $i = 101$ through the proposed data-
 450 driven initialization approach. Posterior computation shows good performance in terms of
 451 mixing, and convergence is assessed after 5,000 Gibbs iterations with a small burn-in of 500.

452 Figure 4 compares true mean and covariance to posterior mean of a select set of com-
 453 ponents of $\Gamma_* = \{\mu(t_i), \Sigma(t_i), i = 101, \dots, 150\}$ including also the 95% hpd intervals. The
 454 results clearly show that the online updating is characterized by a good performance which
 455 allows to capture the behavior of new observations conditioning on the previous estimates.
 456 Note that the posterior distribution of the approximated mean and covariance functions
 457 tends to slightly over-estimate the patterns of the functions at sharp changes, however also
 458 in these cases the true values are within the bands of the credibility intervals. Finally note

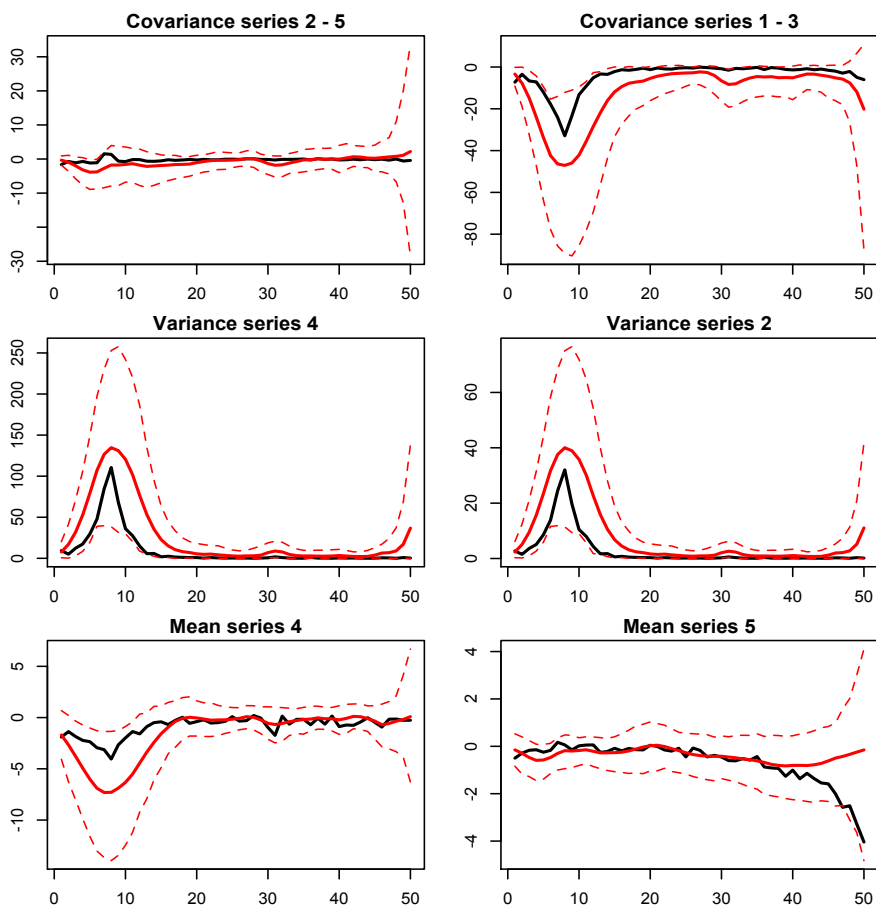


Figure 4: Plots of truth (black) and posterior mean of the online updating procedure (solid red line) for selected components of the covariance (top), variance (middle), mean (bottom). The dotted lines represent the 95% highest posterior density intervals.

459 that the data-driven initialization ensures a good behavior at the beginning of the series,
 460 while the results at the end have wider uncertainty bands as expected.

461 5. Application Study

462 Spurred by the recent growth of interest in the dynamic dependence structure between
 463 financial markets in different countries, and in its features during the crises that have
 464 followed in recent years, we applied our LAF to the multivariate time series of the main
 465 national stock market indices.

466 5.1 National Stock Indices (NSI), Introduction and Motivation

467 National Stock Indices represent technical tools that allow, through the synthesis of numer-
 468 ous data on the evolution of the various stocks, to detect underlying trends in the financial
 469 market, with reference to a specific basis of currency and time. More specifically, each

470 Market Index can be defined as a weighted sum of the values of a set of national stocks,
 471 whose weighting factors is equal to the ratio of its market capitalization in a specific date
 472 and overall of the whole set on the same date.

473 In this application we focus our attention on the multivariate weekly time series of the
 474 main 33 (i.e. $p = 33$) National Stock Indices from 12/07/2004 to 25/06/2012. Figure 5 shows
 475 the main features in terms of stationarity, mean patterns and volatility of two selected NSI
 476 downloaded from <http://finance.yahoo.com/>. The non-stationary behavior, together
 477 with the different bases of currency and time, motivate the use of logarithmic returns
 478 $y_{ji} = \log(I_{ji}/I_{ji-1})$, where I_{ji} is the value of the National Stock Index j at time t_i . Beside
 479 this, the marginal distribution of log returns shows heavy tails and irregular cyclical trends in
 480 the nonparametric estimation of the mean, while EWMA estimates highlight rapid changes
 481 of volatility during the financial crises observed in the recent years. All these results,
 482 together with large settings and high frequency data typical in financial fields, motivate
 483 the use of our approach to obtain a better characterization of the time-varying dependence
 484 structure among financial markets.

485 5.2 LAF for National Stock Index (NSI)

486 We consider the heteroscedastic model $y_i \sim N_{33}(\mu(t_i), \Sigma(t_i))$ for $i = 1, \dots, 415$ and t_i in
 487 the discrete set $\mathcal{T}_o = \{1, 2, \dots, 415\}$, where the elements of $\Gamma = \{\mu(t_i), \Sigma(t_i), 1 = 1, \dots, 415\}$,
 488 defined by (7a)-(7b), are induced by the dynamic latent factor model outlined in 5 and 6.

489 Posterior computation is performed by first rescaling the predictor space \mathcal{T}_o to $(0, 1]$ and
 490 using the same setting of the first simulation study, with the exception of the truncation
 491 levels fixed at $K^* = 4$ and $L^* = 5$ (which we found to be sufficiently large from the fact
 492 that the last few columns of the posterior samples for Θ assumed values close to 0) and
 493 the hyperparameters of the nGP prior for each $\xi_{lk}(t)$ and $\psi_k(t)$ with $l = 1, \dots, L^*$ and
 494 $k = 1, \dots, K^*$, set to $a_\xi = a_A = a_\psi = a_B = 2$ and $b_\xi = b_A = b_\psi = b_B = 5 \times 10^7$ to capture
 495 also rapid changes in the mean functions according to Figure 5. Missing values in our dataset
 496 do not represent a limitation since the Bayesian approach allows us to update our posterior
 497 considering solely the observed data. We run 10,000 Gibbs iterations with a burn-in of 2,500.
 498 Examination of trace plots of the posterior samples for $\Gamma = \{\mu(t_i), \Sigma(t_i), i = 1, \dots, 415\}$
 499 showed no evidence against convergence.

500 Posterior distributions for the variances in Figure 6 demonstrate that we are clearly
 501 able to capture the rapid changes in the dynamics of volatility that occur during the world
 502 financial crisis of 2008, in early 2010 with the Greek debt crisis and in the summer of 2011
 503 with the financial speculation in government bonds of European countries together with the
 504 rejection of the U.S. budget and the downgrading of the United States rating. Moreover,
 505 the resulting marginal distribution of the log returns induced by the posterior mean of $\mu_j(t)$
 506 and $\Sigma_{jj}(t)$, shows that we are also able to accommodate heavy tails as well as mean patterns
 507 cycling irregularly between slow and more rapid changes.

508 Important information about the ability of our model to capture the evolution of world
 509 geo-economic structure during different finance scenarios are provided in Figures 7 and 8.
 510 From the correlations between NASDAQ and the other National Stock Indices (based on
 511 the posterior mean $\{\hat{\Sigma}(t_i)\}_{i=1}^{415}$ of the covariances function) in Figure 7, we can immediately
 512 notice the presence of a clear geo-economic structure in world financial markets (more

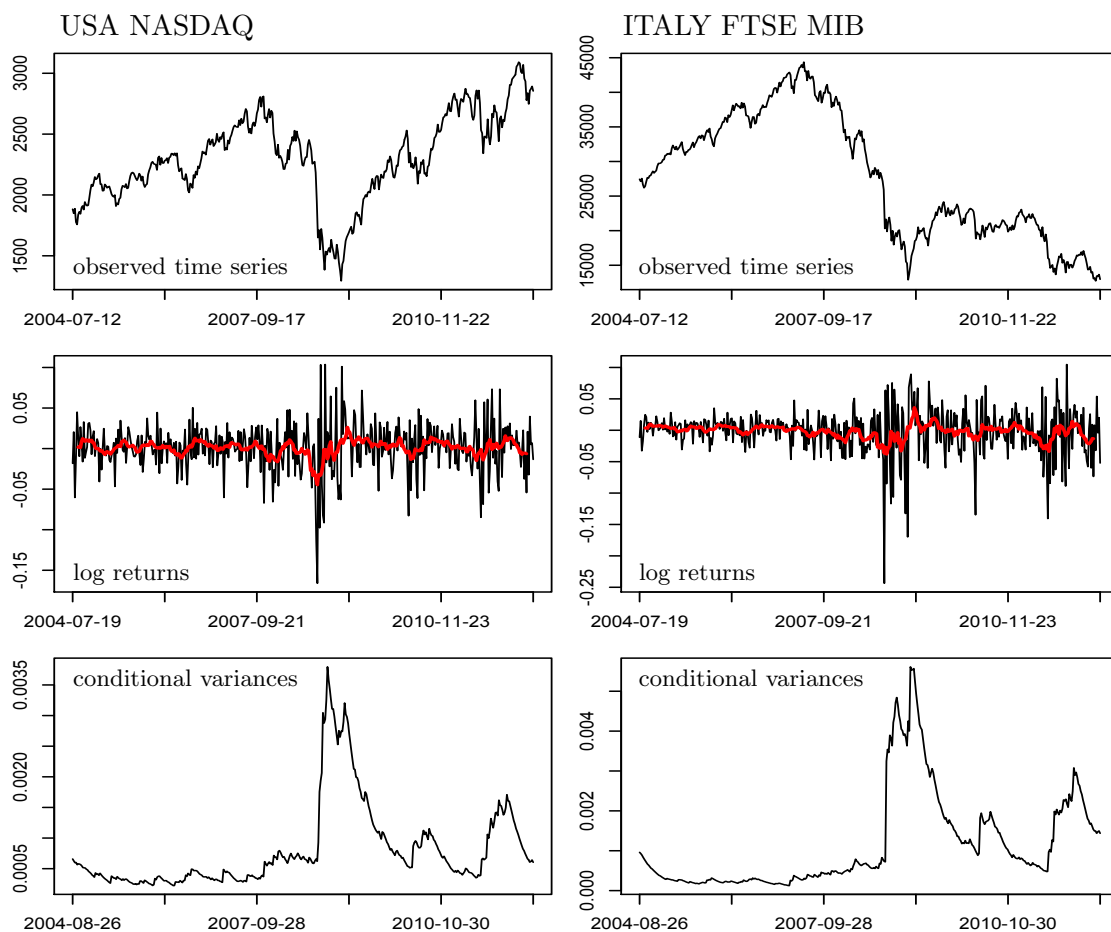


Figure 5: Plots of the main features of USA NASDAQ (left) and ITALY FTSE MIB (right). Specifically: observed time series (top), log-returns series (middle) with nonparametric mean estimation via 12 week Equally Weighted Moving Average (red) in the middle, EWMA volatility estimates (bottom).

513 evident in LAF than in BCR), where the dependence between the U.S. and European
 514 countries is systematically higher than that of South East Asian Nations (Economic Tigers),
 515 showing also different reactions to crises. Plots at the top of the Figure 8 confirms the above
 516 considerations showing how Western countries exhibit more connection with countries closer
 517 in terms of geographical, political and economic structure; the same holds for Eastern
 518 countries where we observe a reversal of the colored curves. As expected, Russia is placed
 519 in a middle path between the two blocks. A further element that our model captures
 520 about the structure of the markets is shown in the plots at the bottom of Figure 8. The
 521 time-varying regression coefficients obtained from the standard formulas of the conditional
 522 normal distribution based on the posterior mean of $\Gamma = \{\mu(t_i), \Sigma(t_i), i = 1, \dots, 415\}$ highlight
 523 clearly the increasing dependence of European countries with higher crisis in sovereign debt
 524 and Germany, which plays a central role in Eurozone as expected.

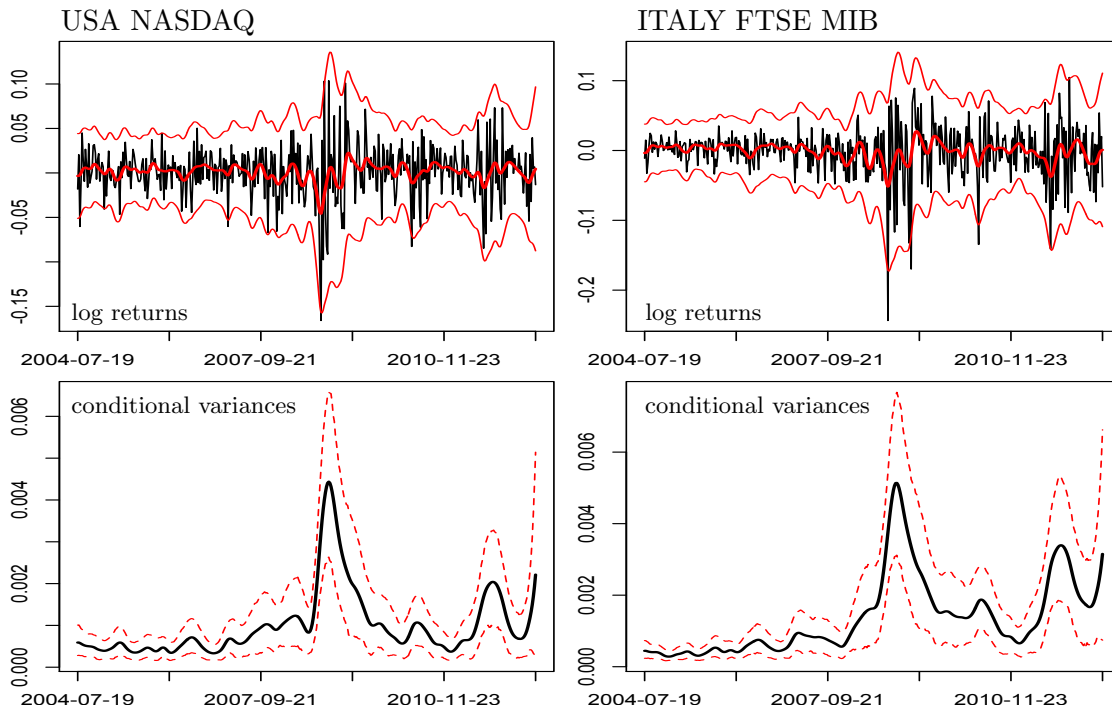


Figure 6: Top: Plot for 2 NSI, respectively USA NASDAQ (left) and ITALY FTSE MIB (right), of the log returns (black) and the time-varying estimated mean $\{\hat{\mu}_j(t_i)\}_{i=1}^{415}$ together with the time-varying 2.5% and 97.5% quantiles (red) of the marginal distribution of y_{ji} from LAF. Bottom: posterior mean (black) and 95% hpd (dotted red) for the variances $\{\Sigma_{jj}(t_i)\}_{i=1}^{415}$.

525 The flexibility of the proposed approach and the possibility of accommodating varying
 526 smoothness in the trajectories over time, allow us to obtain a good characterization of
 527 the dynamic dependence structure according with the major theories on financial crisis.
 528 Top plot in Figure 7 shows how the change of regime in correlations occurs exactly in
 529 correspondence to the burst of the U.S. housing bubble (A), in the second half of 2006.
 530 Moreover we can immediately notice that the correlations among financial markets increase
 531 significantly during the crises, showing a clear international financial contagion effect in
 532 agreement with other theories on financial crisis (see, e.g., Baig and Goldfajn, 1999, and
 533 Claessens and Forbes, 2009). As expected the persistence of high levels of correlation
 534 is evident during the global financial crisis between late-2008 and end-2009 (C), at the
 535 beginning of which our approach also captures a sharp variation in the correlations between
 536 the U.S. and Economic Tigers, which lead to levels close to those of Europe. Further rapid
 537 changes are identified in correspondence of Greek crisis (D), the worsening of European
 538 sovereign-debt crisis and the rejection of the U.S. budget (F) and the recent crisis of credit
 539 institutions in Spain together with the growing financial instability Eurozone (G). Finally,
 540 even in the period of U.S. financial reform launched by Barack Obama and EU efforts to
 541 save Greece (E), we can notice two peaks representing respectively Irish debt crisis and
 542 Portugal debt crisis. Note also that BCR, as expected, tends to over-smooth the dynamic
 543 dependence structure during the financial crisis, proving to be not able to model the sharp

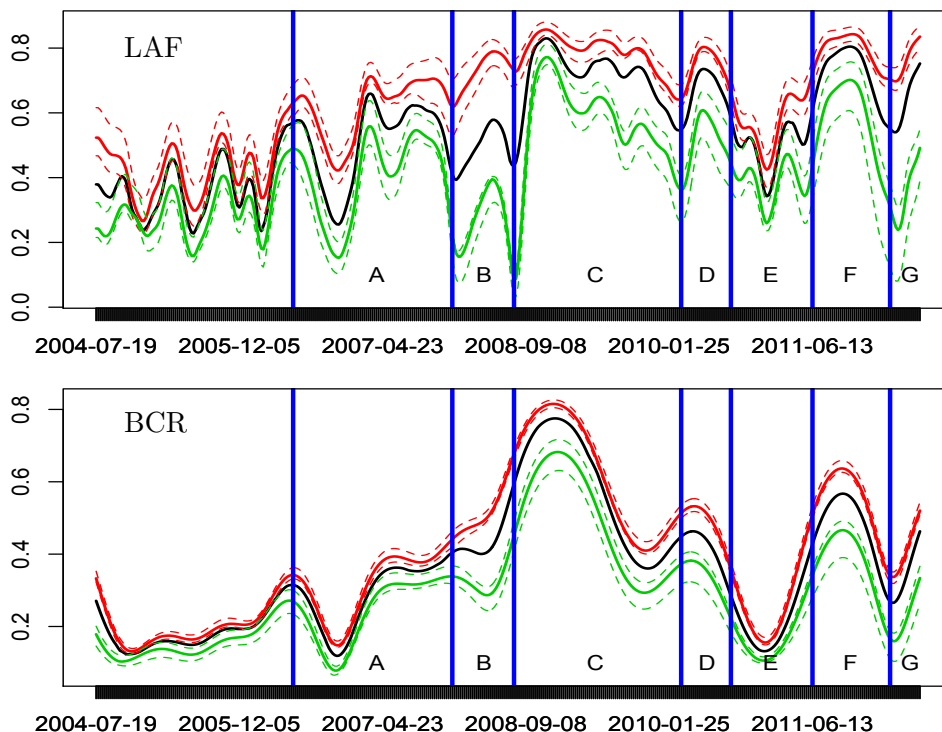


Figure 7: Black line: For USA NASDAQ median of correlations with the other 32 NSI based on posterior mean of $\{\Sigma(t_i)\}_{i=1}^{415}$. Red lines: 25%, 75% (dotted lines) and 50% (solid line) quantiles of correlations between USA NASDAQ and European countries (without considering Greece and Russia which present a specific pattern). Green lines: 25%, 75% (dotted lines) and 50% (solid line) quantiles of correlations between USA NASDAQ and the countries of Southeast Asia (Asian Tigers and India). Timeline: (A) burst of U.S. housing bubble; (B) risk of failure of the first U.S. credit agencies (Bear Stearns, Fannie Mae and Freddie Mac); (C) world financial crisis after the Lehman Brothers' bankruptcy; (D) Greek debt crisis; (E) financial reform launched by Barack Obama and EU efforts to save Greece (the two peaks represent respectively Irish debt crisis and Portugal debt crisis); (F) worsening of European sovereign-debt crisis and the rejection of the U.S. budget; (G) crisis of credit institutions in Spain and the growing financial instability of the Eurozone.

544 change in the correlations between USA NASDAQ and Economic Tigers during late-2008,
 545 and the two peaks representing respectively Irish and Portugal debt crisis at the beginning
 546 of 2011.

547 **5.3 National Stock Indices, Updating and Predicting**

548 The possibility to quickly update the estimates and the predictions as soon as new data
 549 arrive, represents a crucial aspect to obtain quantitative informations about the future
 550 scenarios of the crisis in financial markets. To answer this goal, we apply the online updating
 551 algorithm presented in subsection 3.3, to the new set of weekly observations $\{y_i\}_{i=416}^{422}$ from
 552 02/07/2012 to 13/08/2012 conditioning on posterior estimates of the Gibbs sampler based

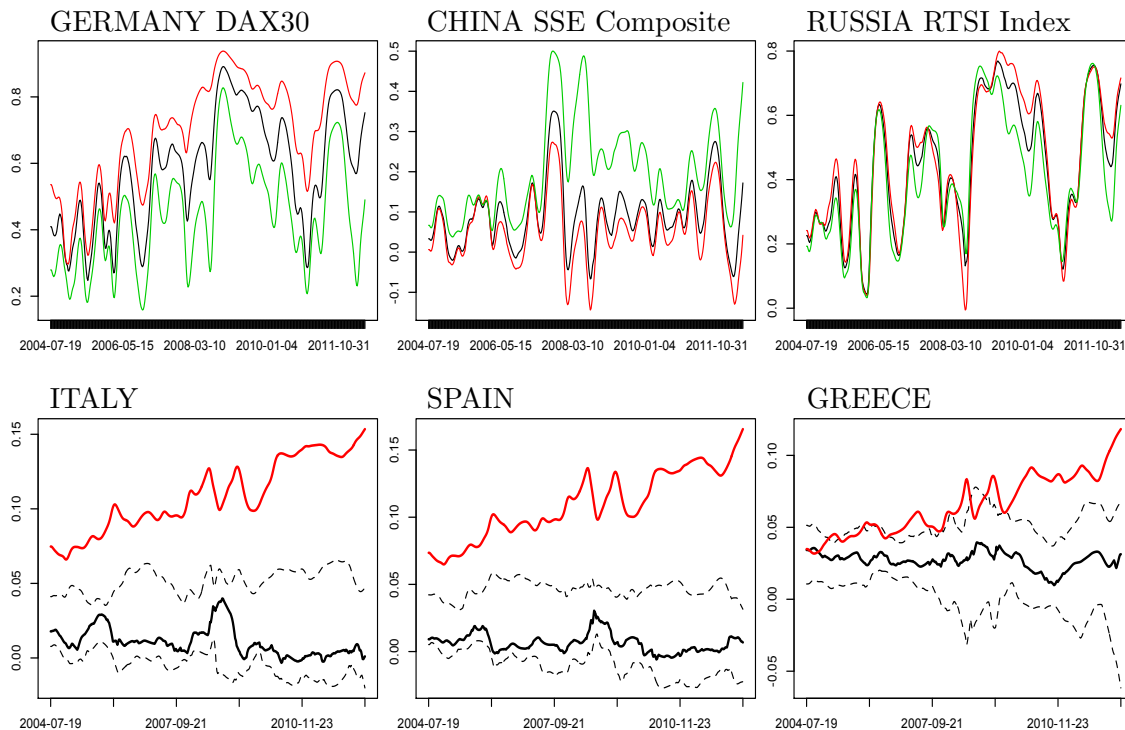


Figure 8: Top: For 3 selected stock market indices, plot of the median of the correlation based on posterior mean of $\{\Sigma(t_i)\}_{i=1}^{415}$ with the other 32 world stock indices (black), the European countries without considering Greece and Russia (red) and the Asian Tigers including India (green). Bottom: For 3 of the European countries more subject to sovereign debt crisis, plot of 25th, 50th and 75th quantiles of the time-varying regression parameters based on posterior mean $\{\hat{\Sigma}(t_i)\}_{i=1}^{415}$ with the other countries (black) and Germany (red).

553 on observations $\{y_i\}_{i=1}^{415}$ available up to 25/06/2012. We initialized the simulation smoother
 554 algorithm with the last 8 observations of the previous sample.

555 Plots at the top of Figure 9 show, for 3 selected National Stock Indices, the new observed
 556 log returns $\{y_{ji}\}_{i=416}^{422}$ (black) together with the mean and the 2.5% and 97.5% quantiles of the
 557 marginal distribution (red) and conditional distribution (green) of $y_{ji}|y_i^{-j}$ with $y_i^{-j} =$
 558 $\{y_{qi}, q \neq j\}$. We use standard formulas of the multivariate normal distribution based on
 559 the posterior mean of the updated $\Gamma_* = \{\mu(t_i), \Sigma(t_i), i = 416, \dots, 422\}$ after 5,000 Gibbs
 560 iterations with a burn in of 500. This is sufficient for convergence based on examining
 561 trace plots of the time-varying mean and covariance matrices. From these results, we can
 562 clearly notice the good performance of our proposed online updating algorithm in obtaining
 563 a characterization for the distribution of new observations. Also note that the multivariate
 564 approach together with a flexible model for the mean and covariance, allow for significant
 565 improvements when the conditional distribution of an index given the others are analyzed.

566 To obtain further informations about the predictive performance of our LAF, we can
 567 easily use our online updating algorithm to obtain h step-ahead predictions for $\Gamma_{T+h|T} =$
 568 $\{\mu(t_{T+h|T}), \Sigma(t_{T+h|T}), h = 1, \dots, H\}$. In particular, referring to Durbin and Koopman

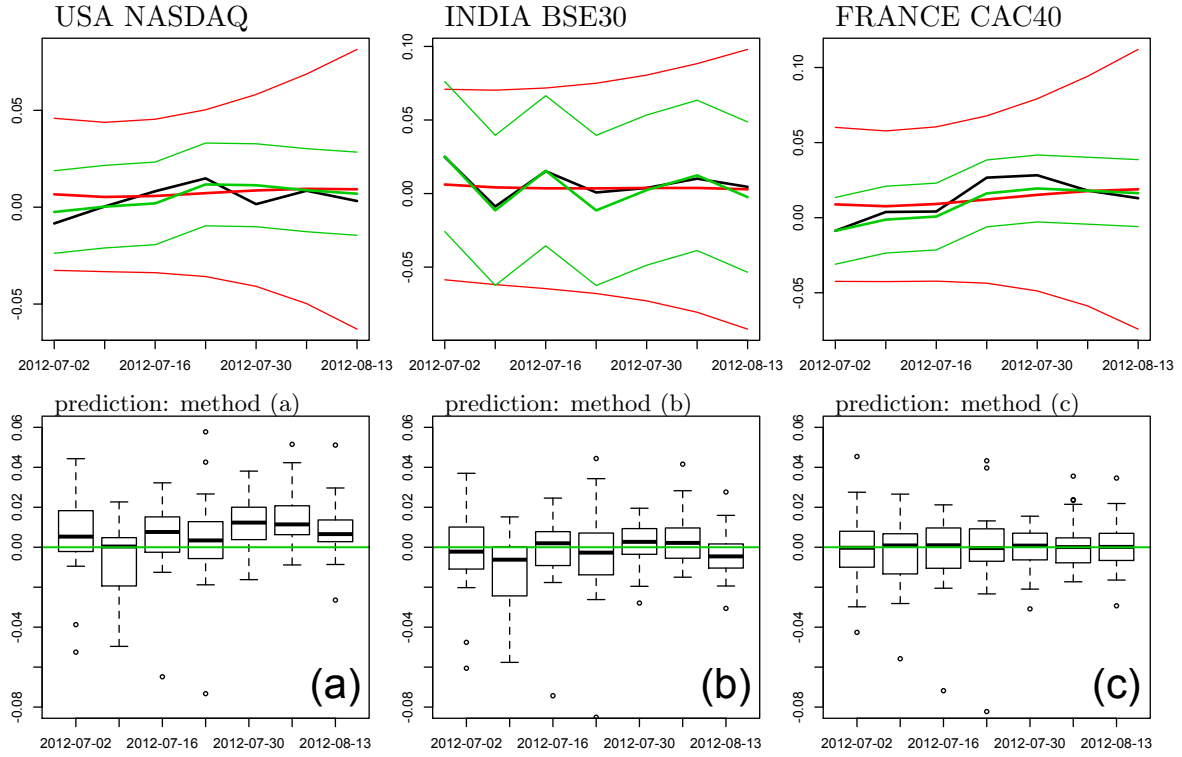


Figure 9: Top: For 3 selected NSI, respectively USA NASDAQ (left), INDIA BSE30 (middle) and FRANCE CAC40 (right), plot of the observed log returns (black) together with the mean and the 2.5% and 97.5% quantiles of the marginal distribution (red) and conditional distribution given the other 32 NSI (green) based on the posterior mean of $\Gamma_* = \{\mu(t_i), \Sigma(t_i), i = 416, \dots, 422\}$ from the online updating procedure for the new observations from 02/07/2012 to 13/08/2012. Bottom: boxplots of the one step ahead prediction errors for the 33 NSI, where the predicted values are respectively: (a) unconditional mean $\{\tilde{y}_{i+1}\}_{i=415}^{421} = 0$, (b) marginal mean of the one step ahead predictive distribution using the online updating procedure for $\{\tilde{y}_{i+1|i}\}_{i=415}^{421}$, (c) conditional mean given the log returns of the other 32 NSI at $i + 1$ of the one step ahead predictive distribution using the online updating procedure for $\{\tilde{y}_{i+1|i}\}_{i=415}^{421}$. Predictions for (b) and (c) are induced by the posterior mean of $\{\mu(t_{i+1|i}), \Sigma(t_{i+1|i}), i = 415, \dots, 421\}$ of our LAF.

569 (2001), we can generate posterior samples of $\Gamma_{T+H|T}$ merely by treating $\{y_i\}_{i=T+1}^{T+H}$
 570 as missing values in the proposed online updating algorithm. Here, we consider the one step ahead
 571 prediction (i.e. $H = 1$) problem for the new observations. More specifically, for each i from
 572 415 to 421, we update the mean and covariance functions conditioning on informations up to
 573 t_i through the online algorithm and then obtain the predicted posterior distribution for
 574 $\Sigma(t_{i+1|i})$ and $\mu(t_{i+1|i})$ by adding to the sample considered for the online updating a last
 575 column y_{i+1} of missing values.

576 Plots at the bottom of Figure 9, show the boxplots of the one step ahead prediction
 577 errors for the 33 NSI obtained as the difference between the predicted value $\tilde{y}_{j,i+1|i}$ and, once
 578 available, the observed log return $y_{j,i+1}$ with $i+1 = 416, \dots, 422$ corresponding to weeks from
 579 02/07/2012 to 13/08/2012. In (a) we forecast the future log returns with the unconditional
 580 mean $\{\tilde{y}_{i+1}\}_{i=415}^{421} = 0$, which is what is often done in practice under the general assumption

581 of zero mean, stationary log returns. In (b) we consider $\tilde{y}_{i+1|i} = \hat{\mu}(t_{i+1|i})$, the posterior
 582 mean of the one step ahead predictive distribution of $\mu(t_{i+1|i})$, obtained from the previous
 583 proposed approach after 5,000 Gibbs iteration with a burn in of 500. Finally in (c) we
 584 suppose that the log returns of all National Stock Indices except that of country j (i.e., $y_{j,i+1}$)
 585 become available at t_{i+1} and, considering $y_{i+1|i} \sim N_p(\hat{\mu}(t_{i+1|i}), \hat{\Sigma}(t_{i+1|i}))$ with $\hat{\mu}(t_{i+1|i})$
 586 and $\hat{\Sigma}(t_{i+1|i})$ posterior mean of the one step ahead predictive distribution respectively for
 587 $\mu(t_{i+1|i})$ and $\Sigma(t_{i+1|i})$, we forecast $\tilde{y}_{j,i+1}$ with the conditional mean of $y_{j,i+1}$ given the other
 588 log returns at time t_{i+1} .

589 Comparing boxplots in (a) with those in (b) we can see that our model allows to obtain
 590 improvements also in terms of prediction. Furthermore, by analyzing the boxplots in (c) we
 591 can notice how our ability to obtain a good characterization of the time-varying covariance
 592 structure can play a crucial role also in improving forecasting, since it enters into the
 593 standard formula for calculating the conditional mean in the normal distribution.

594 6. Discussion

595 In this paper, we have presented a continuous time multivariate stochastic process for
 596 time series to obtain a better characterization for mean and covariance temporal dynamics.
 597 Maintaining simple conjugate posterior updates and tractable computations in moderately
 598 large p settings, our model increases significantly the flexibility of previous approaches as it
 599 captures sharp changes both in mean and covariance dynamics while accommodating heavy
 600 tails. Beside these key advantages, the state space formulation enables development of a
 601 fast online updating algorithm particularly useful for high frequency data.

602 The simulation studies highlight the flexibility and the overall better performance of
 603 LAF with respect to the models for multivariate stochastic volatility most widely used
 604 in practice, both when adaptive estimation techniques are required, and also when the
 605 underlying mean and covariance structures do not show sharp changes in their dynamic.

606 The application to the problem of capturing temporal and geo-economic structure be-
 607 tween the main financial markets demonstrates the utility of our approach and the im-
 608 provements that can be obtained in the analysis of multivariate financial time series with
 609 reference to (i) heavy tails, (ii) locally adaptive mean regression, (iii) sharp changes in co-
 610 variance functions, (iii) high dimensional dataset, (iv) online updating with high frequency
 611 data (v) missing values and (vi) predictions. Potentially further improvements are possible
 612 using a stochastic differential equation model that explicitly incorporates prior information
 613 on dynamics.

614 Appendix A1. Posterior Computation

615 For a fixed truncation level L^* and a latent factor dimension K^* the detailed steps of the
 616 Gibbs sampler for posterior computations are:

- 617 1. Define the vector of the latent state and the error terms in the state space equation
 618 resulting from nGP prior for dictionary elements as

$$\begin{aligned} \Xi_i &= [\xi_{11}(t_i), \xi_{21}(t_i), \dots, \xi_{L^*K^*}(t_i), \xi'_{11}(t_i), \dots, \xi'_{L^*K^*}(t_i), A_{11}(t_i), \dots, A_{L^*K^*}(t_i)]^T \\ \Omega_{i,\xi} &= [\omega_{i,\xi_{11}}, \omega_{i,\xi_{21}}, \dots, \omega_{i,\xi_{L^*K^*}}, \omega_{i,A_{11}}, \omega_{i,A_{21}}, \dots, \omega_{i,A_{L^*K^*}}]^T \end{aligned}$$

619 Given Θ , $\{\eta_i\}_{i=1}^T$, $\{y_i\}_{i=1}^T$, Σ_0 and the variances in latent state equations $\{\sigma_{\xi_{lk}}^2\}$,
 620 $\{\sigma_{A_{lk}}^2\}$, with $l = 1, \dots, L^*$ and $k = 1, \dots, K^*$; update $\{\Xi_i\}_{i=1}^T$ by using the simulation
 621 smoother in the following state space model

$$y_i = [\eta_i^T \otimes \Theta, 0_{p \times (2 \times K^* \times L^*)}] \Xi_i + \epsilon_i \quad (9)$$

$$\Xi_{i+1} = T_i \Xi_i + R_i \Omega_{i,\xi} \quad (10)$$

622 Where the observation equation in (9) results by applying the *vec* operator in the
 623 latent factor model $y_i = \Theta \xi(t_i) \eta_i + \epsilon_i$. More specifically recalling the property
 624 $vec(ABC) = (C^T \otimes A)vec(B)$ we obtain

$$\begin{aligned} y_i = vec(y_i) &= vec\{\Theta \xi(t_i) \eta_i + \epsilon_i\} \\ &= vec\{\Theta \xi(t_i) \eta_i\} + vec(\epsilon_i) \\ &= (\eta_i^T \otimes \Theta) vec\{\xi(t_i)\} + \epsilon_i. \end{aligned}$$

625 The state equation in (10) is a joint representation of the equations resulting from the
 626 nGP prior on each ξ_{lk} defined in (3). As a result, the $(3 \times L^* \times K^*) \times (3 \times L^* \times K^*)$ matrix
 627 T_i together with the $(3 \times L^* \times K^*) \times (2 \times L^* \times K^*)$ matrix R_i reproduce, for each dic-
 628 tionary element the state equation in (3) by fixing to 0 the coefficients relating latent
 629 states with different (l, k) (from the independence between the dictionary elements).
 630 Finally, recalling the assumptions on $\omega_{i,\xi_{lk}}$ and $\omega_{i,A_{lk}}$, $\Omega_{i,\xi}$ is normally distributed with
 631 $E[\Omega_{i,\xi}] = 0$ and $E[\Omega_{i,\xi} \Omega_{i,\xi}^T] = \text{diag}(\sigma_{\xi_{11}}^2 \delta_i, \sigma_{\xi_{21}}^2 \delta_i, \dots, \sigma_{\xi_{L^*K^*}}^2 \delta_i, \sigma_{A_{11}}^2 \delta_i, \sigma_{A_{21}}^2 \delta_i, \dots, \sigma_{A_{L^*K^*}}^2 \delta_i)$.

632 2. Given $\{\Xi_i\}_{i=1}^T$ sample each $\sigma_{\xi_{lk}}^2$ and $\sigma_{A_{lk}}^2$ respectively from

$$\begin{aligned} \sigma_{\xi_{lk}}^2 | \{\Xi_i\} &\sim \text{InvGa} \left(a_\xi + \frac{T}{2}, b_\xi + \frac{1}{2} \sum_{i=1}^{T-1} \frac{(\xi'_{lk}(t_{i+1}) - \xi'_{lk}(t_i) - A_{lk}(t_i) \delta_i)^2}{\delta_i} \right) \\ \sigma_{A_{lk}}^2 | \{\Xi_i\} &\sim \text{InvGa} \left(a_A + \frac{T}{2}, b_A + \frac{1}{2} \sum_{i=1}^{T-1} \frac{(A_{lk}(t_{i+1}) - A_{lk}(t_i))^2}{\delta_i} \right) \end{aligned}$$

633

634 3. Similarly to Ξ_i and $\Omega_{i,\xi}$ let

$$\begin{aligned} \Psi_i &= [\psi_1(t_i), \psi_2(t_i), \dots, \psi_{K^*}(t_i), \psi'_1(t_i), \dots, \psi'_{K^*}(t_i), B_1(t_i), \dots, B_{K^*}(t_i)]^T \\ \Omega_{i,\psi} &= [\omega_{i,\psi_1}, \omega_{i,\psi_2}, \dots, \omega_{i,\psi_{K^*}}, \omega_{i,B_1}, \omega_{i,B_2}, \dots, \omega_{i,B_{K^*}}]^T \end{aligned}$$

635 be the vectors of the latent state and error terms in the state space equation resulting
 636 from nGP prior for ψ . Conditional on Θ , $\{\xi(t_i)\}_{i=1}^T$, $\{y_i\}_{i=1}^T$, Σ_0 , and the variances
 637 in latent state equations $\{\sigma_{\psi_k}^2\}$, $\{\sigma_{B_k}^2\}$, with $k = 1, \dots, K^*$; sample $\{\Psi_i\}_{i=1}^T$ from the
 638 simulation smoother in the following state space model

$$y_i = [\Theta \xi(t_i), 0_{p \times (2 \times K^*)}] \Psi_i + \varpi_i, \quad (11)$$

$$\Psi_{i+1} = G_i \Psi_i + F_i \Omega_{i,\psi}, \quad (12)$$

639 $\varpi_i \sim N(0, \Theta \xi(t_i) \xi(t_i)^T \Theta^T + \Sigma_0)$. The observation equation in (11) results by marginal-
 640 izing out ν_i in the latent factor model with nonparametric mean regression $y_i =$

641 $\Theta\xi(t_i)\psi(t_i) + \Theta\xi(t_i)\nu_i + \epsilon_i$. Analogously to Ξ_i , the state equation in (12) is a joint
 642 representation of the state equation induced by the nGP prior on each ψ_k defined in
 643 (4); where the $(3 \times K^*) \times (3 \times K^*)$ matrix G_i and the $(3 \times K^*) \times (2 \times K^*)$ matrix F_i are
 644 constructed with the same goal of the matrices T_i and R_i in the state space model for
 645 Ξ_i . Finally, $\Omega_{i,\psi} \sim N_{2 \times K^*}(0, \text{diag}(\sigma_{\psi_1}^2 \delta_i, \sigma_{\psi_2}^2 \delta_i, \dots, \sigma_{\psi_{K^*}}^2 \delta_i, \sigma_{B_1}^2 \delta_i, \sigma_{B_2}^2 \delta_i, \dots, \sigma_{B_{K^*}}^2 \delta_i))$.

646 4. Given $\{\Psi_i\}_{i=1}^T$ update each $\sigma_{\psi_k}^2$ and $\sigma_{B_k}^2$ respectively from

$$\begin{aligned} \sigma_{\psi_k}^2 | \{\Psi_i\} &\sim \text{InvGa} \left(a_\psi + \frac{T}{2}, b_\psi + \frac{1}{2} \sum_{i=1}^{T-1} \frac{(\psi'_k(t_{i+1}) - \psi'_k(t_i) - B_k(t_i)\delta_i)^2}{\delta_i} \right) \\ \sigma_{B_k}^2 | \{\Psi_i\} &\sim \text{InvGa} \left(a_B + \frac{T}{2}, b_B + \frac{1}{2} \sum_{i=1}^{T-1} \frac{(B_k(t_{i+1}) - B_k(t_i))^2}{\delta_i} \right) \end{aligned}$$

647

648 5. Conditioned on $\Theta, \Sigma_0, y_i, \xi(t_i)$ and $\psi(t_i)$, and recalling $\nu_i \sim N_{K^*}(0, I_{K^*})$; the standard
 649 conjugate posterior distribution $\nu_i | \Theta, \Sigma_0, \tilde{y}_i, \xi(t_i), \psi(t_i)$ is

$$N_{K^*} \left((I + \xi(t_i)^T \Theta^T \Sigma_0^{-1} \Theta \xi(t_i))^{-1} \xi(t_i)^T \Theta^T \Sigma_0^{-1} \tilde{y}_i, (I + \xi(t_i)^T \Theta^T \Sigma_0^{-1} \Theta \xi(t_i))^{-1} \right)$$

650 with $\tilde{y}_i = y_i - \Theta\xi(t_i)\psi(t_i) = \Theta\xi(t_i)\nu_i + \epsilon_i$.

651 6. Conditioned on $\Theta, \{\eta_i\}_{i=1}^T, \{y_i\}_{i=1}^T$, and $\{\xi(t_i)\}_{i=1}^T$ (obtained from Ξ_i), the standard
 652 conjugate posterior from which to update σ_j^{-2} is

$$\sigma_j^{-2} | \Theta, \{\eta_i\}, \{y_i\}, \{\xi(t_i)\} \sim \text{Ga} \left(a_\sigma + \frac{T}{2}, b_\sigma + \frac{1}{2} \sum_{i=1}^T (y_{ji} - \theta_j \xi(t_i) \eta_i)^2 \right)$$

653 Where $\theta_j = [\theta_{j1}, \dots, \theta_{jL^*}]$

654 7. Given $\{\eta_i\}_{i=1}^T, \{y_i\}_{i=1}^T, \{\xi(t_i)\}_{i=1}^T$ and the hyperparameters ϕ and τ the shrinkage prior
 655 on Θ combined with the likelihood for the latent factor model lead to the Gaussian
 656 posterior

$$\theta_j | \{\eta_i\}, \{y_i\}, \{\xi(t_i)\}, \phi, \tau \sim N_{L^*} \left(\tilde{\Sigma}_\theta \tilde{\eta}^T \sigma_j^{-2} \begin{bmatrix} y_{j1} \\ \vdots \\ y_{jT} \end{bmatrix}, \tilde{\Sigma}_\theta \right)$$

where $\tilde{\eta}^T = [\xi(t_1)\eta_1, \xi(t_2)\eta_2, \dots, \xi(t_T)\eta_T]$ and

$$\tilde{\Sigma}_\theta^{-1} = \sigma_j^{-2} \tilde{\eta}^T \tilde{\eta} + \text{diag}(\phi_{j1}\tau_1, \dots, \phi_{jL^*}\tau_{L^*})$$

657

658 8. The Gamma prior on the local shrinkage hyperparameter ϕ_{jl} implies the standard
 659 conjugate posterior given θ_{jl} and τ

$$\phi_{jl} | \theta_{jl}, \tau \sim \text{Ga} \left(2, \frac{3 + \tau \theta_{jl}^2}{2} \right)$$

660 9. Conditioned on Θ and τ , sample the global shrinkage hyperparameters from

$$\begin{aligned} \vartheta_1 | \Theta, \tau^{(-1)} &\sim \text{Ga} \left(a_1 + \frac{pL^*}{2}, 1 + \frac{1}{2} \sum_{l=1}^{L^*} \tau_l^{(-1)} \sum_{j=1}^p \phi_{jl} \theta_{jl}^2 \right) \\ \vartheta_h | \Theta, \tau^{(-h)} &\sim \text{Ga} \left(a_2 + \frac{p(L^* - h + 1)}{2}, 1 + \frac{1}{2} \sum_{l=1}^{L^*} \tau_l^{(-h)} \sum_{j=1}^p \phi_{jl} \theta_{jl}^2 \right) \end{aligned}$$

661 Where $\tau_l^{(-h)} = \prod_{t=1, t \neq h}^l \vartheta_t$ for $h = 1, \dots, p$

662 10. Given the posterior samples from Θ , Σ_0 , $\{\xi(t_i)\}_{i=1}^T$ and $\{\psi(t_i)\}_{i=1}^T$ the realization of
663 the LAF process for $\{\mu(t_i), \Sigma(t_i), t_i \in \mathcal{T}\}$ conditioned on the data $\{y_i\}_{i=1}^T$ is

$$\begin{aligned} \mu(t_i) &= \Theta \xi(t_i) \psi(t_i) \\ \Sigma(t_i) &= \Theta \xi(t_i) \xi(t_i)^T \Theta^T + \Sigma_0. \end{aligned}$$

664 Appendix B. Online Updating Algorithm

665 Consider Θ , Σ_0 , $\{\sigma_{\xi_{lk}}^2\}$, $\{\sigma_{A_{lk}}^2\}$, $\{\sigma_{\psi_k}^2\}$ and $\{\sigma_{B_k}^2\}$ fixed at their posterior mean $\hat{\Theta}$, $\hat{\Sigma}_0$, $\{\hat{\sigma}_{\xi_{lk}}^2\}$,
666 $\{\hat{\sigma}_{A_{lk}}^2\}$, $\{\hat{\sigma}_{\psi_k}^2\}$, $\{\hat{\sigma}_{B_k}^2\}$ respectively, and let $\hat{\Xi}_T$, $\hat{\Sigma}_{\Xi_T}$ and $\hat{\Psi}_T$, $\hat{\Sigma}_{\Psi_T}$ be the sample mean and
667 covariance matrix of the posterior distribution respectively for Ξ_T and Ψ_T obtained from
668 the posterior estimates of the Gibbs sampler conditioned on $\{y_i\}_{i=1}^T$.

669 1. Given $\hat{\Theta}$, $\hat{\Sigma}_0$, $\{\hat{\sigma}_{\xi_{lk}}^2\}$, $\{\hat{\sigma}_{A_{lk}}^2\}$, $\{\eta_i\}_{i=T+1}^{T+H}$ and $\{y_i\}_{i=T+1}^{T+H}$ update $\{\Xi_i\}_{i=T+1}^{T+H}$ by using the
670 simulation smoother in the following state space model

$$\begin{aligned} y_i &= [\eta_i^T \otimes \hat{\Theta}, 0_{p \times (2 \times K^* \times L^*)}] \Xi_i + \epsilon_i \\ \Xi_{i+1} &= T_i \Xi_i + R_i \Omega_{i,\xi} \end{aligned}$$

671 Where Ξ_{T+1} can be initialized from the standard one step ahead predictive distribu-
672 tion for the state space model $\Xi_{T+1} \sim \text{N}(T_T \hat{\Xi}_T, T_T \hat{\Sigma}_{\Xi_T} T_T^T + R_T E[\Omega_{T,\xi} \Omega_{T,\xi}^T] R_T^T)$

673 2. Conditioned on $\hat{\Theta}$, $\hat{\Sigma}_0$, $\{\hat{\sigma}_{\psi_k}^2\}$, $\{\hat{\sigma}_{B_k}^2\}$, $\{\xi(t_i)\}_{i=T+1}^{T+H}$ and $\{y_i\}_{i=T+1}^{T+H}$ sample $\{\Psi_i\}_{i=T+1}^{T+H}$
674 through the simulation smoother in the state space model

$$\begin{aligned} y_i &= [\hat{\Theta} \xi(t_i), 0_{p \times (2 \times K^*)}] \Psi_i + \varpi_i \\ \Psi_{i+1} &= G_i \Psi_i + F_i \Omega_{i,\psi} \end{aligned}$$

675 Similarly to Ξ_{T+1} , $\Psi_{T+1} \sim \text{N}(G_T \hat{\Psi}_T, G_T \hat{\Sigma}_{\Psi_T} G_T^T + F_T E[\Omega_{T,\psi} \Omega_{T,\psi}^T] F_T^T)$

676

677 3. Given $\hat{\Theta}$, $\hat{\Sigma}_0$, $\{y_i\}$, $\xi(t_i)$ and $\psi(t_i)$, for $i = T+1, \dots, T+H$, sample ν_i from the standard
678 conjugate posterior distribution for $\nu_i | \Theta, \Sigma_0, \tilde{y}_i, \xi(t_i), \psi(t_i)$:

$$N_{K^*} \left((I + \xi(t_i)^T \Theta^T \Sigma_0^{-1} \Theta \xi(t_i))^{-1} \xi(t_i)^T \Theta^T \Sigma_0^{-1} \tilde{y}_i, (I + \xi(t_i)^T \Theta^T \Sigma_0^{-1} \Theta \xi(t_i))^{-1} \right)$$

679 with $\tilde{y}_i = y_i - \Theta \xi(t_i) \psi(t_i) = \Theta \xi(t_i) \nu_i + \epsilon_i$.

680

681 4. Compute the updated covariance $\{\Sigma(t_i)\}_{i=T+1}^{T+H}$ and mean $\{\mu(t_i)\}_{i=T+1}^{T+H}$ from the usual
 682 equations

$$\begin{aligned}\Sigma(t_i) &= \hat{\Theta}\xi(t_i)\xi(t_i)^T\hat{\Theta}^T + \hat{\Sigma}_0 \\ \mu(t_i) &= \hat{\Theta}\xi(t_i)\psi(t_i)\end{aligned}$$

683 Acknowledgments

684 This research was partially supported by grant R01ES17240 from the National Institute of
 685 Environmental Health Sciences (NIEHS) of the National Institutes of Health (NIH) and by
 686 grant CPDA097208/09 from the University of Padua, Italy.

687 References

- 688 Aguilar, O., & West, M. (2000). Bayesian dynamic factor models and portfolio allocation.
 689 *Journal of Business & Economic Statistics* 18, 338–357.
- 690 Alexander, C.O. (2001). Orthogonal GARCH. *Mastering Risk* 2, 21–38.
- 691 Baig, T., & Goldfajn, I. (1999). Financial Market Contagion in the Asian Crisis. *Staff*
 692 *Papers, International Monetary Fund* 46, 167–195.
- 693 Bhattacharya, A., & Dunson, D.B. (2011). Sparse Bayesian infinite factor models.
 694 *Biometrika* 98, 291–306.
- 695 Bollerslev, T., Engle, R.F., & Wooldridge, J.M. (1988). A capital-asset pricing model with
 696 time-varying covariances. *Journal of Political Economy* 96, 116–131.
- 697 Bru, M. (1991). Wishart Processes. *Journal of Theoretical Probability* 4, 725–751.
- 698 Burns, P. (2005). Multivariate GARCH with Only Univariate Estimation.
 699 <http://www.burns-stat.com>.
- 700 Carvalho, C.M., Lucas, J.E., Wang, Q., Chang, J., Nevins, J.R., & West, M. (2008). High-
 701 dimensional sparse factor modeling - Applications in gene expression genomics. *Journal*
 702 *of the American Statistical Association* 103, 1438–1456.
- 703 Claessens, S., & Forbes, K. (2009) International Financial Contagion, An overview of the
 704 Issues. Springer.
- 705 Ding, Z. (1994). Time series analysis of speculative returns. PhD thesis, University of
 706 California, San Diego.
- 707 Donoho, D.L., & Johnstone, J.M. (1994). Ideal spatial adaptation by wavelet shrinkage.
 708 *Biometrika* 81, 425–455.
- 709 Donoho, D.L., & Johnstone, J.M. (1995). Adapting to unknown smoothness via wavelet
 710 shrinkage. *Journal of the American Statistical Association* 90, 1200–1224.

- 711 Durbin, J., & Koopman, S. (2001). *Time Series Analysis by State Space Methods*. Oxford
712 University Press Inc., New York.
- 713 Durbin, J. and Koopman, S. (2002). A simple and efficient simulation smoother for state
714 space time series analysis. *Biometrika* 89, 603–616.
- 715 Engle, R.F., & Kroner, K.F. (1995). Multivariate simultaneous generalized ARCH. *Econo-*
716 *metric Theory* 11, 122–150.
- 717 Engle, R.F. (2002). Dynamic conditional correlation: a simple class of multivariate gener-
718 alized autoregressive conditional heteroskedasticity models. *Journal of Business & Eco-*
719 *nomics Statistics* 20, 339–350.
- 720 Fan, J. & Gijbels, I. (1995). Data-driven bandwidth selection in local polynomial fitting:
721 variable bandwidth and spatial adaptation. *Journal of the Royal Statistical Society* 57,
722 371–394.
- 723 Fox, E., & Dunson, D.B. (2011). Bayesian Nonparametric Covariance Regression.
724 *arXiv:1101.2017*.
- 725 Friedman, J. H. (1991). Multivariate Adaptive Regression Splines. *Annals of Statistics* 19,
726 1–67.
- 727 Gelman, A., & Rubin, D.B. (1992). Inference from iterative simulation using multiple
728 sequences. *Statistical Science* 7, 457–511.
- 729 George, E.I. & McCulloch, R.E. (1993). Variable selection via Gibbs sampling. *Journal of*
730 *the American Statistical Association* 88, 881–889.
- 731 Geweke, J., & Zhou, G. (1996). Measuring the pricing error of the arbitrage pricing theory.
732 *Review of Financial Studies* 9, 557–587.
- 733 Ghosh, J., & Dunson, D.B. (2009) Default priors and efficient posterior computation in
734 Bayesian factor analysis. *Journal of Computational and Graphical Statistics* 18, 306–
735 320.
- 736 Hastie, T. J. & Tibshirani, R. J. (1990). *Generalized Additive Models*. London: Chapman
737 and Hall.
- 738 Huang, J.Z., Wu, C.O & Zhou, L. (2002). Varying-coefficient models and basis function
739 approximations for the analysis of repeated measurements. *Biometrika* 89, 111–128.
- 740 Kalman, R.E. (1960). A new approach to linear filtering and prediction problems. *Journal*
741 *of Basic Engineering* 82, 35–45.
- 742 Lopes, H.F., & West, M. (2004). Bayesian model assessment in factor analysis. *Statistica*
743 *Sinica* 14, 41–67.
- 744 Lopes, H. F., Salazar, E., & Gamerman, D. (2008) Spatial Dynamic Factor Analysis
745 *Bayesian Analysis* 3, 759–792.

- 746 Lopes, H.F., Gamerman, D., & Salazar, E. (2011) Generalized spatial dynamic factor
747 models. *Computational Statistics & Data Analysis* 55, 1319–1330.
- 748 Nakajima, J., & West, M. (2012) Dynamic factor volatility modeling: A Bayesian latent
749 threshold approach *Journal of Financial Econometrics* in press.
- 750 Pati D., Bhattacharya A., Pillai N.S., & Dunson D.B. (2012). Bayesian high-dimensional
751 covariance matrix estimation. <http://ftp.stat.duke.edu/WorkingPapers/12-05.html>.
- 752 Rasmussen, C.E. & Williams, C.K.I (2006). *Gaussian processes for machine learning*.
753 Boston: MIT Press.
- 754 Smith, M. & Kohn, R. (1996). Nonparametric regression using Bayesian variable selection.
755 *Journal of Econometrics* 75, 317-343.
- 756 Tsay, R.S. (2005). *Analysis of Financial Time Series*. II ed., Wiley.
- 757 van der Weide, R. (2002). GO-GARCH: a multivariate generalized orthogonal GARCH
758 model. *Journal of Applied Econometrics* 17, 549–564.
- 759 West, M. (2003). Bayesian factor regression models in the large p , small n paradigm.
760 *Bayesian Statistics* 7, 723–732.
- 761 Wilson, A.G. & Ghahramani Z. (2010). Generalised Wishart Processes. *arXiv:1101.0240*.
- 762 Wolpert, R.L., Clyde M.A. & Tu, C. (2011). Stochastic expansions using continuous dic-
763 tionaries: Levy adaptive regression kernels. *Annals of Statistics* 39, 1916–1962.
- 764 Wu C.O., Chiang C.T. & Hoover D.R. (1998). Asymptotic confidence regions for kernel
765 smoothing of a varying-coefficient model with longitudinal data. *Journal of the American*
766 *Statistical Association* 93,1388-1402 .
- 767 Zhu, B., & Dunson, D.B. (2012). Locally Adaptive Bayes Nonparametric Regression via
768 Nested Gaussian Processes. *arXiv:1201.4403*.